DOI: 10.1002/ ((please add manuscript number))
Article type: Review

Advanced Functional Composite Materials Towards E-skin for Health Monitoring and Artificial Intelligence

Qi-Jun Sun, Qin-Teng Lai, Zhenhua Tang, Xin-Gui Tang, Xin-Hua Zhao*, and Vellaisamy A. L. Roy**

Dr. Q.-J. Sun, Mr. Q.-T. Lai, Dr. Z. Tang, Prof. X.-G. Tang
School of Physics and Optoelectric Engineering
Guangdong University of Technology
Guangzhou, 511400, P. R. China
E-mail: tangzh@gdut.edu.cn

Dr. X.-H. Zhao
Department of Chemistry
South University of Science and Technology of China
Shenzhen 518055, P. R. China
E-mail: zhaoxinhualuky@126.com

Prof. V. A. L. Roy
James Watt School of Engineering
University of Glasgow
Glasgow, G12 8QQ, United Kingdom
E-mail: Roy.Vellaisamy@glasgow.ac.uk

Keywords: functional composites, flexible sensors, E-skin, health monitoring, artificial intelligence

Abstract: Electronic skin (E-skin), especially the wearable sensors efficiently detect various stimuli attracted huge research interest owing to their potential applications in health monitoring and artificial intelligence. On the other hand, functional polymer composites (FPC) possessing excellent properties such as light weight, good flexibility and superior electrical performances, are promising candidates as building blocks for flexible electronics. Accordingly, tremendous efforts have been devoted to the development of polymer composites with functional properties for E-skin applications. Here, we review recent advances on the controlled fabrication of various fillers based functional polymer composites and their diverse applications in E-skin. In addition, contemporary studies on fabrication strategies, working mechanisms, and device performance for E-skin based on the functional polymer composites are reviewed,

including flexible pressure sensors, strain sensors, temperature sensors, energy harvesters and transistors. Furthermore, the applications of functional composite based flexible electronics in healthcare and artificial intelligence are discussed. Finally, the existing challenges and opportunities for the functional composite materials based E-skin are summarized.

1. Introduction

In recent years, flexible and wearable electronics have attracted worldwide research interests due to their promising potentials in medical diagnosis, prosthetics, and artificial intelligence.[1-4] Particularly, the flexible and wearable sensors can be employed as wearables to collect physiological signals including human body motions, wrist pulses, body temperature, and electrocardiograph (ECG) signals, where these detections provide vital information in disease prediction and diagnosis.[5-9] Apart from the emerging demands of flexible sensors in health monitoring, there is urgent need for functional sensors for smart robotics.[10-12] Therefore, it is highly desired to boost up the development and commercialization of flexile sensors for wearable and robotic applications.

Various flexible sensing platforms, such as pressure sensor,[13, 14] strain sensor,[15, 16] temperature sensor,[17-19] self-powered tactile sensor,[20-22] and sensing platforms with multifunctional capabilities[23] have been widely explored over the past decades. For practical applications, excellent mechanical properties and outstanding sensing performance of flexible sensors are necessary. On one hand, wearables with direct contact to human skin or utilized as electronic skin (E-skin), the sensors should own the superior properties of light weight, good flexibility, stretchability and biocompatibility. On the other hand, high sensitivity and fast response of the flexible sensors are highly required for accurate detection of external stimuli. Consequently, to obtain flexible electronic materials and sensors with superior mechanical properties, composite materials become an excellent option because they can be engineered.[24, 25] Compared with the other materials, polymer composites are more attractive in building

flexible electronics because of their superior flexibility, good stretchability, and feasibility in functional engineering, enabling them to be the most promising building blocks for the next-generation flexible and wearable electronics. To achieve flexible sensors with excellent sensing properties, abundant strategies have been proposed in the construction of the sensor devices in terms of employing sponge microstructures,[26-28] interlocked microstructures,[29-31] and bio-inspired microstructures.[32-34] In merits of the above mentioned superior properties, functional polymer composites based on various fillers have been extensively investigated for E-skins and their applications in health monitoring and artificial intelligence are summarized in **Figure 1**.

In this review, we summarize the recent advances in the rational design and controlled preparation of functional polymer composites for flexible smart sensors in particular. In addition to conductive polymer composites, we comprehensively discuss the semiconducting and insulating group of polymer composites, and their applications in flexible/wearable electronics. Firstly, we discuss the preparations of functional polymer composites based on various fillers including graphene, graphite, carbon blacks (CBs), carbon nanowires (CNWs), carbon nanotubes (CNTs), gold nanowires (AuNWs), copper nanowires (CuNWs), silver nanowires (AgNWs), polymers, and metal oxide nanoparticles. Then, we review the structural design, sensing mechanism and characterization of functional polymer composite based flexible electronics including strain sensors, pressure sensors, temperature sensors, energy harvesters, and thin film transistors. Furthermore, we provide a detailed description of engineering technologies with an emphasis on flexible sensor fabrication and their representative applications in health monitoring (such as wrist pulses, blood pressure, and electrophysiological signals) and as E-skin for smart robots are discussed. Finally, a conclusion is given and future perspectives in the field of functional polymer composites for wearable and portable sensing systems are addressed.

2. Categories of Functional Polymer Composite Materials

According to the electrical conducting properties, polymer composite materials are mainly divided into three types and they are conductors, semiconductors and insulators.[24, 35-37] All these three types of polymer composites have been extensively studied as the candidate materials for building flexible and stretchable electronics. To be an excellent candidate for flexible and wearable electronics, unique properties including excellent flexibility/stretchability, light weight and mechanical/chemical stability are highly required for the composite materials. To achieve these superior properties, tremendous efforts have been devoted to the construction of functional polymer composite materials by selecting proper fillers and appropriate engineering of polymer composites. Varieties of nano-/microstructured materials such as graphene,[38] carbon nanotubes/nanowires,[39-41] metal particles,[42-44] metal nanowires,[45, 46] metal oxide nanoparticles,[30, 47] and polymers[48-50] have been extensively studied as candidate fillers in functional polymer composite. In this section, we report recent advances in the development of functional polymer composite materials with various compositions in terms of the selection criteria of the fillers and property optimization of the polymer composites. Firstly, we introduce representative works of functional polymer composites as conductors, semiconductors and dielectrics for flexible electronics. Recent advances in the development of flexible substrates for flexible sensors can be referred to previously reported review works.[51-53]

The electrical conductivity of stretchable conductors is one of the critical parameters directly associated with the performance of flexible electronics. However, most of the elastomers with desired mechanical properties for electronic device applications are not conductive, hence incorporating conductive nano-/micromaterials into the polymer matrix to obtain the polymer composite conductors became a strategy.[54, 55] For polymer composites, the percolation threshold is the most important parameter in the percolation theory, which is defined as the minimum volume fraction of conductive fillers required to construct continuous electrical pathways in a given composite material. It should be noticed that the percolation threshold only

implies the formation of the electrical conductive pathways rather than the highest conductivity of a given polymer composite. Therefore, a high conductivity of the polymer composite could be achieved by introducing a large amount of conductive filler surpassing the percolation threshold. However, excessive conductive fillers in the polymer matrix usually degrade the flexibility and stretchability of the polymer composite films. Consequently, a tradeoff between the mechanical properties and the electrical conductivity should be considered for diverse applications. Therefore, if there are strict requirements in flexibility, transparency and fabrication cost of the polymer composites, the nano-/micromaterials with a low percolation threshold and low cost are usually selected as the conductive fillers in the polymer composites. In the following section, we introduce and discuss the selection criteria for the representative conductive nano-/micromaterials in terms of their percolation threshold, preparation cost, and physical/chemical properties for conductive polymer composites.

2.1. Conductive Carbon Based Nano-/Micromaterials

Carbon materials including carbon black (CB), graphene, carbon nanotubes (CNTs) and carbon nanowires (CNWs) are at the center of academic and industrial research over the past years due to their excellent electrical conductivity, superior mechanical properties, and relatively low fabrication cost.[56-60] Incorporated into the polymer matrix, the physical and chemical properties of the carbon materials could be mostly maintained while imparting the polymer matrix with an improved electrical conductivity.

2.1.1. CBs and Graphite

CBs and graphite-based nano-/micromaterials have been widely studied as candidate fillers in conductive polymer composites.[61] For example, Chen et al. reported the coated CBs on commercially available rubber band to realize a conductive and flexible composite via a cost-efficient fabrication approach as shown in **Figure 2a**.[62] As depicted in the SEM images in Figure 2a, the CBs could be uniformly distributed on the surface of a rubber band to form the

conductive CBs/rubber composite. To obtain conductive polymer composite film with microstructures for strain sensors, CBs, sodium chloride (NaCl) and thermoplastic urethane elastomer (TPU) were mixed thoroughly to get the conductive printable ink, and the porous polymer composite with hierarchical structures were obtained via a 3D printing approach reported by Wang et al.[63] Meanwhile, the conductivity of the microstructured composite film found to have correlation with CB concentrations in the composite inks. Although this kind of polymer composite is not suitable as conductive electrodes in flexible electronics because of its relatively low conductivity, introducing porous microstructures into the polymer composite enables the film with a desired pressure response for low-power tactile sensors. Compared with CBs, graphite-based nano-/micromaterials show an improved electrical conductivity due to the ordered arrangement of the carbon atoms in graphite. Yokota et al. reported graphite based polymer composite for temperature sensor arrays based on the positive temperature coefficient (PTC) effect in conductive filler-based polymer composites.[64] Based on the composite, the sensor can detect temperatures over a large area with high spatial resolution up to 0.1 °C and high sensitivity. In our previous work, graphite micro-sheets were mixed with polydimethylsiloxane (PDMS) to obtain the conductive composite ink and hierarchically microstructured composite films were achieved by roller bar-assisted printing with the commercially available sandpaper as the template. The conductivity of the polymer composite films could be well controlled by altering the concentrations of the graphite in the composite inks.[65] However, because of its large percolation threshold, a large amount of graphite is required to fill in the composite ink to achieve an ideal conductivity, which results in a degraded flexibility. In order to improve the flexibility while maintaining a good conductivity of the graphite/PDMS based composite film, graphite powder, NaCl and PDMS prepolymer were thoroughly mixed to obtain the functional composite ink. A flexible, hierarchically structured composite sponge was achieved via employing the sandpaper template and NaCl sacrificial template. The flexibility and conductivity of the composite films were investigated

by changing the ratios of graphite and NaCl in the composite inks.[66] As shown in Figure 2b, the composite film was fabricated for temperature sensing and pressure sensing, showing good temperature sening ability. The above results imply that the electrical conductivity of the CB or graphite particle networks mainly depends on the reorganization of the inter-particle contacts within the composites. Because of their relatively high percolation thresholds, it is difficult to employ the CB or graphite fillers in polymer matrix as electrodes for ultra-flexible electronics. Alternatively, the introduction of the porous microstructures inside the polymer composites can improve their flexibility and enable them with a good response to the external forces for low-power flexible sensors.

2.1.2. Graphene Based Fillers

Compared with CBs and graphite, graphene based conductive fillers in the forms of nanosheets and 3D structures have obtained much more attentions due to their excellent conductivity, flexibility and light weight. Since the discovery of graphene by Novoselov and Geim in 2004, graphene attracted extensive research interest as a potential electronic material due to its unique physical properties.[67, 68] The abundant delocalized electrons impart the graphene with extraordinary electrical properties, where the concentration of electrons and holes can be as high as 10^{13} cm^{-2}, endowing it with a high mobility of 200,000 cm^2 V^{-1} s^{-1}. These unique properties enable graphene to be ideal conductive filler in the functional polymer composites. Recently, varieties of strategies have been proposed by the researchers in developing graphene (including graphene and reduced graphene oxide) based polymer composites. For example, Zhao et al. reported a reduced graphene oxide (rGO) and polyimide (PI) composite foam prepared via a two-step fabrication process for self-powered flexible sensors as shown in Figure 2c.[69] As depicted in the SEM images in Figure 2c, the rGO/PI foam revealed hierarchical porous structures which were produced in the freeze-drying process and the layered constructions between rGO sheets. The graphene fillers have a low percolation

threshold and excellent electrical conductivity, which allow the related polymer composites with excellent flexibility and conductivity.

Fractured microstructure design for conductive polymer composite sponge was reported by Yu et al.[70] In order to construct a large-scale conductive sponge with dense and fractured microstructures, graphene nanosheets were employed as conductive coatings on a commercial polyurethane (PU) sponge. Taking advantages of excellent conductivity of graphene nanosheets, and the feasibility in deformation of the PU sponge with external forces, a flexible, conductive graphene/PU composite with fractured hierarchical microstructures was developed via a simple dip coating strategy.

Thanks to the relatively low percolation threshold and excellent electrical conductivity, the functional polymer composites based on graphene or rGO fillers could be employed as electrodes for stretchable electronics and pressure-sensitive films of flexible tactile sensors. In the future, realizing large-scale synthesis of cost-effective graphene and developing new fabrication strategies of graphene filler based functional polymer composite would further extend their practical applications in the field of flexible electronics.

2.1.3 CNTs Based Fillers

Among the carbon nano-/micro-materials, carbon nanotubes are the most promising candidates to obtain the percolation networks within the composites because of their large aspect ratios. Additionally, the length and electrical conductivity of the CNTs could be controlled by adjusting the fabrication strategies for different applications.[57, 71] Furthermore, CNT based polymer composites with functional microstructures can be achieved via templated growth or materials engineering technologies.[72-76] In 2014, Park et al. developed a functional composite film with interlocked microdomes based on CNT fillers.[77] The defining feature of their design is the shaping of the composite film with regular microdome arrays by coating PDMS/CNTs composite ink onto a silicon mold (Figure 2d). The microstructured composite film was fabricated by the micro-molding process, and the microstructures were characterized by SEM

as depicted in Figure 2d. As the conductivity of the functional polymer composite film was sensitive to the external pressures, two composite films were combined together for flexible tactile sensors. A pressure-sensitive functional composite film with regular micro-patterns was fabricated in this work. However, the microdoms were fabricated on the silicon template which was developed by the complicated and expensive lithography process. In the future, achieving large-area preparation of CNTs with controlled structures using a simple approach and realizing the functional polymer composite films via a cost-effective strategy may promote the performance and extend the practical applications of CNT filler based polymer composites. In brief, the carbon-based nanocomposites have great potential in low-cost flexible sensors.

2.2. Metallic Fillers

Metal-based nanomaterials in diverse forms of particles, nanowires and nanosheets are emerging as efficient conductive filling material because of their inherently good electrical conductivity as well as excellent mechanical properties.[78-83] Similar with that of the carbon-based fillers, the electrical conductivity of the metal percolation networks is closely related with the shape and aspect ratio of the metallic fillers. Recently, many wet chemical approaches have been reported for the controlled synthesis of metal-based conductive fillers with diverse structures. Similarly, a large amount of metal particles are required to form the conductive pathways within the composite because of their relatively high percolation threshold. The poor compatibility between polymer matrix and metal nanoparticles typically lead to nanoparticle aggregation before the volume fraction of the metal particle fillers reaching the percolation threshold. Thus, implanting or blending of prefabricated metal nanoparticles within the polymer matrix has so far not proven successful in preparing flexible conductive composite film. Alternative approaches are to synthesize metal nanoparticles with sea-urchin shaped structures, flower-like structures or in-situ fabrication of metal nanoparticles embedded in the polymer to obtain the functional polymer composite.[44]

2.2.1. Metallic Nanoparticles

In order to low the percolation threshold of metallic nanoparticles in polymer matrix, Lee et al. demonstrated a highly transparent, conductive composite composed of sea-urchin shaped metal nanoparticles (SSNPs) and polyurethane (PU) matrix as illustrated in **Figure 3a**.[44] Firstly, they synthesized SSNPs by using tetrachloroauric(III) acid trihydrate ($HAuCl_4 \cdot 3H_2O$) and silver nitrate ($AgNO_3$) and the shape and size of the SSNPs were easily tuned by controlling the relative ratio of silver and gold ions. SSNPs with long spikes were successfully obtained by optimizing the relative ratio of silver and gold ions. This work demonstrated that shapes of the long spikes and electrical conductance can well maintained by covering the SSNPs within TPP. The SEM image of SSNPs in the PU elastomer is depicted in Figure 3a, indicating an average diameter and spike length of 110 and 50 nm, respectively. To fabricate the conductive SSNPs/PU composite film, they first dispersed small quantity of SSNPs into the PU prepolymer followed by adding the relevant PU curing agent into the mixture of SSNPs and PU prepolymer, followed by a spin-coating process to obtain a SSNPs/PU composite film. The effect of doping concentration on thin film optical transparency was also investigated, revealing that the composite film showed superior optical transparency with a low SSNPs concentration. In this work, they successfully reduced the percolation threshold of the metallic nanoparticles by employing the spike-shaped nanostructures to obtain highly flexible and transparent conductive polymer composite. In future, the spike-shaped metal particles could be broadly used in the stretchable and wearable sensors if they could be synthesized in mass production via a low-cost fabrication method.

As an example, Wang *et al.* fabricated a highly conductive and fluorine-free superhydrophobic conductive elastomer composites (CEC) by a novel “ion reduction and simultaneous molecule phase separation” method.[84] Figure 3b shows the SEM images of CEC surface and cross-section morphology, high-resolution transmission electron microscope images (TEM) of AgNP@OCA, aggregates of Ag and their corresponding elemental mapping images. Xu *et al*. prepared an antibacterial multifunctional conductive rubber film based on Ag-NP for strain

sensors.[85] Before the critical in-situ reduction of silver nanoparticles, carboxylated styrene butadiene rubber (XSBR)/CA film was first prepared. Then, the final conductive rubber film is completed by introducing $AgNO_3$ into the CA phase, in which Ag NP is reduced in situ to construct a conductive path. The schematic diagram of the preparation process of XSBR/CA/Ag film is shown in Figure 3c. Employing the in-situ preparation approach to fabricate the metal nanoparticles can greatly reduce the percolation threshold in the polymer matrix, which can achieve the uniform distribution of metal nanoparticle in the polymer composite.

2.2.2. Metal Plate Based Fillers

Owing to their excellent conductivity, metal nanosheet (MNs) and nanofilms (MFs) based polymer composites have been widely investigated as electrodes in the development of flexible electronics.[86-88] Additionally, the MNs- and MFs-based polymer composites could be used as active layers for flexible physical and biological sensors via material engineering.[89] Recently, various strategies have been proposed to fabricate the MNs- and MFs-based polymer composites, and their applications for mechanical sensors have been demonstrated.[90] For example, Zhang et al. deposited Au thin film on regularly patterned PDMS substrate to obtain the Au/PDMS polymer composite and its application for piezoresistive pressure sensory system has been demonstrated. In another example, an electrically conductive composite based on Ag flakes fillers was demonstrated by Guo et al.[91] The conductivity of the composite was close to that of bulk metals and could be well maintained while stretching. The resistivity change of the polymer composite was about 3 times of original values under a strain of 119%, indicating a good stability to the external strain. Compared with the metal nanoparticles, metal plate shows improved conductivity in the polymer composites. However, similar with the carbon-based fillers, the MNs have low aspect ratios and large amount of metal fillers are required to form the conducting pathways inner the composites, which consequently decreases the flexibility of the composites.

2.2.3. Metal Nanowire Based Fillers

Alternatively, metal nanowires (such as AuNWs, CuNWs and AgNWs) have recently attracted wide research attention thanks to their high aspect ratio, good conductivity and ductility.[92] Despite the low production during the synthesis and high cost of AuNWs, they show excellent stability to oxidation. Recently, Cheng's group has demonstrated the vertically aligned AuNWs (V-AuNWs) based polymer composite for flexible pressure sensors.[93] The V-AuNWs microarrays were developed via a modified seed mediated growth at room temperature on PDMS films with pyramidal microstructures and the fabrication process is schematically shown in Figure 3d. As shown in the digital photo and SEM image in Figure 3d, a conformal thin layer of AuNWs was obtained on the PDMS film after the growth of AuNWs. The as-prepared freestanding AuNWs/PDMS composite film exhibited excellent flexibility and bonding between AuNWs and the PDMS substrate.

Among the representative metallic NWs, CuNWs have the highest susceptibility to oxidation, but the preparation cost is relatively low owing to their natural abundance. Accordingly, various nanocomposites film with CuNWs as conductive fillers have been reported. For example, CuNWs with high aspect ratio were synthesized by Wang et al. and employed as fillers in the thermal transporting composite for the first time.[94] The thermal conductivity of the composite with various CuNWs volume fractions was investigated. A good thermal conductivity of 2.46 W/mK was achieved at a low loading fraction of 0.9 vol%, which was attributed to the high thermal conductivity and low percolation threshold for the long-aspect-ratio CuNWs in the polymer nanocomposites. As an another example, a porous bulk 3D CuNW based sponge composite was obtained by directly growing CuNW hydrogel network out from the precursor solution.[95] Furthermore, the above report demonstrated that the electrical and mechanical properties of the CuNW based composite could be adjusted by tuning the concentration of the reaction precursor, growth time and temperature of the synthesis process,

proving a feasible strategy to obtain CuNWs filler based polymer composites for various applications.

Compared with the AuNWs and CuNWs, AgNWs are the best candidate as conductive fillers in the polymer composite due to their excellent electrical conductivity, mass production, and reasonable production cost. As a result, various approaches have been raised by the researchers in the development of AgNWs filler based polymer composites. For example, a highly stretchable microstructured AgNWs/elastomer composite film based wearable strain sensor was presented by Kim et al.[96] The surface microstructures were easily prepared by drop-casting the AgNWs onto the silicon template with valley structures. The densely packed microprism-array architecture of the composite film leads to a large morphological change in the AgNWs percolation network by efficiently concentrating the strain in the valley regions upon stretching (Figure 3e). Meanwhile, the percolation network comprising AgNWs with a high aspect ratio was stable enough to prevent electrical failure, even under high strains. This enabled the developed sensors to simultaneously satisfy high sensitivity (gauge factor = 81 at 130% strain) and high stretchability (150%) while ensuring long-term reliability (10000 cycles at 150% strain). On the other hand, AgNWs/ poly(vinylidene fluoride) (PVDF) composite nanofibers were prepared by Cho's group via electrospinning (Figure 3f).[45] Polar crystalline β-phase of PVDF is realized in the electrospinning process due to the generated uniaxial stretching of the polymer. The β-phase crystal formation was further enhanced by the addition of AgNWs owing to the electrostatic interactions between the AgNWs and dipoles of the PVDF chains. Addition of AgNWs enhanced the charge trapping of the induced charges, so the composite nanofibers were then employed as the triboelectric layer for triboelectric nanogenerators (TENG). The performance of the TENG devices are greatly improved in both the surface charge potential and the charge trapping capability of the nanofibrous triboelectric film, demonstrating the potential of AgNW-based composite film for high-performance TENG devices.

2.2.4. Metal Oxide Based Fillers

Because of their distinctive electrical and piezoelectric properties, metal oxide nanomaterials such as ZnO,[97, 98] $BaTiO_3$,[99] and $ZnSnO_3$[100, 101] have been incorporated into various polymers as one of promising platforms for flexible energy harvesters. For example, Chun et al. developed a highly stretchable composite film composed of the regularly arranged piezoelectric hemispheres and PDMS matrix.[102] The key novelty of their design is that they developed the highly-arranged piezoelectric hemispheres in PDMS matrix. The fabrication procedure is schematically illustrated in **Figure 4a**. In detail, an aqueous suspension of polystyrene (PS) beads was employed to obtain closely packed monolayer template on UV/Ozone treated SiO_2/Si substrate. ZnO or piezoelectric lead zirconate titante (PZT) film was then deposited on the PS spheres by magnetron sputtering process, followed by thermally annealled in air to burnout the PS spheres and crystallize the films simultaneously. After that, PDMS prepolymer was then poured onto the PS sphere template and developed into a free-standing film after thermal annealing, achieving the crescent-shaped PDMS film after removing the PS spheres by acetone as shown in Figure 4b and c. Shi et al. reported a $BaTiO_3$/PDMS polymer composite for energy harvesters (Figure 4d-f).[103] The addition of $BaTiO_3$ nanoparticles in the PDMS enhanced the Young Modulus of the nanocomposites, resulting in an enhanced output performance of the nanogenerators. Recently, Li et al. fabricated a flexible zinc oxide/poly(vinylidene fluoride) (ZnO/PVDF) nanocomposite film by electrospinning technology for nanogenerators.[97] A detailed flow diagram fabrication of ZnO/PVDF polymer composite film is presented in Figure 4g. In brief, the ZnO NPs and ZnO NRs are mixed into the PVDF prepolymer under continuous stirring simultaneously. The polymer solution was then electronspun onto a rotating disk to obtain the polymer composite film. The optical and SEM images of the nanocomposite fibrous membrane are presented in Figure 4g, showing the homogeneous fabrication of the polymer composite films. Currently, the challenge in fabrication of metal oxide/polymer composite film is the issue of metal oxide nanoparticle

aggregation in polymers composite, which needs to be resolved by material engineering techniques.

2.3. Polymer Based Fillers

Owing to the carrier transporting capability of conductive domain and the excellent mechanical flexibility of polymer chain, conducting polymers have been broadly utilized as conductors in flexible electronics and sensors. The representative conducting polymers that are used as flexible conductors include polypyrrole (PPy), polyaniline (PANI), poly(3,4-ethylenedioxythiophene): polystyrene sulfonate (PEDOT:PSS).[104-110] It should be noted that the traditional conductive polymers usually exhibit poor stretchability and mixing with stretchable polymer to obtain the functional polymer composites has been demonstrated as an efficient strategy to extend their stretchable applications. Recently, a PPy/PDMS composite film with surface wrinkling microstructures has been fabricated by Yang et al. As shown in **Figure 5a,** the in situ wrinkling was achieved during the oxidative polymerization growth of PPy film on flexible PDMS substrate in an acidic solution.[109] A third surface wrinkling was induced by further heating/cooling processing, demonstrating a controlled formation of three-scale nested wrinkling microstructures for flexible electronics (Figure 5b).

In the past decades, E-skin has been widely explored owing to its promising application in healthcare monitoring and artificial intelligence.[111-113] Along with flexibility and stretchability, self-repairing capability of E-skin is another fascinating property for practical applications. Moreover, self-repairing capability can greatly improve the durability of flexible electronics and lengthen the corresponding lifetime for practical use. Unfortunately, despite a variety of strategies have been proposed in the development of E-skin, the self-healing property has been proved as a great challenge in E-skin development.[114-116] Therefore, it is highly desired to impart the self-repairing capability to the functional composite materials for E-skin and bio-inspired soft robots. The common route to fabricate the conductive polymer composite for flexible electronics is by incorporating the conductive fillers into a self-repairing capability

network, nonetheless the stretchability of the electronics degrades a lot.[117] Above study reported a more straight approach to develop the self-repairing polymer composite by synthesizing self-healing electronic materials with high stretchability. Recently, based on polyacrylic acid, polyaniline, and phytic acid, Wang et al. have achieved a ternary polymer composite with excellent electrical conductivity of 0.12 S cm^{-1}, high stretchability of 500% and good self-healing properties.[118] In particular, both the mechanical property and electrical conductivity could be recovered with about 99% efficiency within 24 h, which was enabled by electrostatic interaction and dynamic hydrogen bonding in the polymer composite. As depicted in Figure 5c, the PA molecules in the polymer composite could built hydrogen bonding and afford electrostatic interaction with PANI chains as well as dopants.[118] The electrostatic interactions and noncovalent hydrogen bonding are crucial for self-healing property of the polymer composite, restoring mechanical and electrical properties in ambient condition.[119–121] Additionally, the mechanical energy under stretching could be well dissipated because of the weak electrostatic forces and hydrogen bonds, allowing for an excellent stretchability of the polymer composite. It should be mentioned that the presence of water was essential to enable the self-healing function because the hydrogen bonds might be destroyed if the polymer is under anhydrous condition. As shown in Figure 5d, the as-prepared polymer films exhibited outstanding mechanical properties including high stretchability and flexibility because of the porous structure in the polymer composite film. Meanwhile, the photographs in Figure 5d demonstrate that the polymer film under stretched condition (200%) is still with good conductivity, showing that the prepared polymer composite film has high stretchability and intrinsic conductivity as well. Furthermore, this synthetic method was solution-processed, which was compatible with inexpensive, large-area manufacturing process. To prove its self-healing ability, the film was cut into three pieces and the fresh cuts were kept into contact with mild pressure. The breaking points could successfully self-heal in 24 h and the mechanical properties could be well recovered and maintained even after couples of breaking/healing

cycles.

3. Approaches to Fabricate the Functional Polymer Composites

In this section, we review and analyze the commonly used technologies in the development of functional polymer composites as film, fiber, sponge, etc. for flexible electronics and sensors.[122, 123] Additionally, we discuss each method with regard to their advantages and drawbacks, and representative examples are also introduced.

3.1. Thermal evaporation

Thermal evaporation is a useful technology to deposit semiconductors and metal electrodes by using shadow masks in the fabrication of organic light-emitting diodes (OLEDs), organic field-effects transistors (OFETs), and optical electronics.[14, 124] This technology is also used in the fabrication of functional polymer composite materials. For instance, Pang et al. deposited a thin layer of Pt onto high-aspect-ratio nanofibers by thermal evaporation to obtain the electrically conductive and mechanically flexible composite for highly sensitive strain sensors.[79] The strain sensor was fabricated by the interlocking the upper and lower Pt-coated nanofibers to detect the tiny distortion caused by hair-to-hair contact due to the highly sensitive contact-dependent change of the functional polymer composite. Moreover, the thickness of the metal film in the composites could be readily tuned by adjusting the deposition rate and time to obtain composites with different conductivities for the requirements of diverse applications. Furthermore, metal nanoparticles were thermally deposited on the substrate followed by fabricating a thin polymer layer as charge trapping layer for data storage devices.[125, 126] However, high vacuum and sophisticated equipment are required for this technology, which is costly and adverse for mass production.

3.2. Dip-coating

Solution-processing strategies are extensively employed in film preparation due to their advantages of large-scale compatibility in manufacturing compared with the thermal evaporation method. Dip-coating, one of the solution-processing techniques, is a straightforward solution to obtain the functional composite materials in the construction of flexible electronics. Generally, the substrates or support materials are simply dipped into a precursor solution followed by a drying process to get the functional composites. Employing the dip-coating approach, Zhang et al. developed cracked cellulose nanofibril/silver nanowire coated polyurethane sponges for piezoresistive pressure sensors.[127] The photographs and schematic device structure of the pressure sensor arrays are shown in **Figure 6a**. When a weight or ball is put on top of the pressure sensor array, corresponding pressure distributions are clearly revealed via the relative resistance change of every pixel as shown at the bottom of Figure 6a. Wang et al. recently reported an efficient design strategy to fabricate $Ti_3C_2T_x$ MXene/Ni chain/ZnO array hybrid nanostructures on cotton fabrics using a facile dip coating and hydrothermal method for flexible sensors as shown in Figure 6b.[37] The dip-coating approach for functional polymer composite is simple and straightforward, but the uniformity of the composite film needs improvement in the future.

3.3. Spin-coating

Spin-coating as one of the solution-processing methods has been widely adopted in the fabrication of composite film for flexible electronics.[128–134] Lee et al. realized a sea-urchin shaped metal nanoparticles (SSNPs) embedded PU composite film by spin-coating for transparent pressure sensors.[44] For the composite film preparation, a small quantity of SSNPs were firstly dispersed in the PU matrix. After that, the curing agent was added into the mixture of SSNPs and PU followed by deposition onto an ITO/PET substrate by spin-coating. Finally, a transparent and conductive piezoresistive composite film was achieved after thermal annealing. In another example, a ZnO NW/PEDOT:PSS composite was fabricated by spin-coating for

flexible piezo-phototronic pressure mapping sensor matrix (Figure 6c).[135] The pressure sensor array was demonstrated with a high spatial resolution of 7 μm over a wide pressure detection range from 40 to 100 MPa through the controlled growth of the ZnO nanowire array. Furthermore, the spin-coating approach has been used to obtain high-*k* polymer composites as the dielectric for low-power field-effect transistors (FETs) and charge trapping layer for data storage electronics as well.[136, 137] The thickness of the composite film can be readily tuned by controlling the solution concentration and the spin-coating speed. The spin-coating approach is more suitable for the solutions with low viscosity but difficult for the high viscosity solutions to obtain the uniform film. It should be noticed that a uniform dispersion of the functional fillers in the polymer solution is important to obtain the high quality polymer composite films.

3.4. Spray-coating

Spray-coating has been developed to prepare the polymer composite on the flexible substrate. The mixture of the fillers and polymer materials can be dispersed in an aqueous and organic solution. The organic solution is more suitable for the deposition of the polymer composite while the aqueous solution may result in non-uniform films because of the relatively low evaporation speed of the aqueous solvent. The dispersed filler materials in the solution can be loaded in the spray gun and sprayed onto the substrates. As per the schematic illustration in **Figure 7a**, Li et al. fabricated a smart coating with multiwalled carbon nanotubes dispersed in a thermoplastic elastomer solution by spray-coating.[138] It was proved that this coating could impart various substrates with super hydrophobic properties due to the large amount of micrometer-sized features generated in the spraying process, which was verified by the SEM images as shown in Figure 7a. The obtained polymer composite exhibited good responses to bending, stretching and torsion forces, which enabled the functional polymer composite to be applied in flexible tactile sensors. In another example, Chou et al. realized a SWNT/PDMS composite by coating the SWNT on a pyramidal microstructured PDMS as schematically

illustrated in Figure 7b.[139] The SWNT was uniformly spray coated on top of the pyramidal-microstructured PDMS surface to obtain the composite film with low resistance. To tune the conductivity of the composite film, they used kapton tape to remove the SWNT from the top of the pyramid with different forces. Meanwhile, the height of the SWNT on the microstructured PDMS was adjusted as shown in the SEM images (bottom of Figure 7b).

3.5. Printing

Printing has been proved to be a cost-effective approach in achieving high-performance flexible electronics and sensors with a proper processing temperature.[140–142] Printing approaches have the following advantages of reduced material wastage, simple processing technique, and low cost, which makes this technique attractive in building flexible electronics. Generally, the printing approaches can be divided into two main categories: the patterned structures do not contact with the substrate called the noncontact printing and the patterned structures contact with the substrate directly (called the contact printing). In the fabrication of functional polymer composites, both the noncontact and contact printing are widely used.[143, 144]

3.4.1. Screen Printing

Screen printing is one of the noncontact approaches to fabricate flexible electronics. Due to the merits of simple and cost-effective fabrication process, screen printing has been extensively employed to achieve patterned polymer composite film on flexible substrate for sensors. Khan et al developed a large-scale flexible tactile sensor array using screen-printed MWCNT/PDMS composite as shown in **Figure 8a**.[145] In their work, the composite inks with different weight ratios of MWCNT and PDMS were prepared and printed onto pre-printed electrodes on a flexible PET substrate to obtain the piezoresistive composite layer. Subsequently, another piece of PET substrate with screen-printed Ag electrodes was aligned and assembled together with the functional nanocomposite and bottom electrodes to complete the sensor fabrication.

3.4.2. 3D Printing

3D printing is the representative of contact printing, which has emerged as a versatile technique to print thermoplastic polymer composite for diverse architectures which can be readily controlled by computer.[146–150] Recently, Wang et al. have achieved a full 3D printed stretchable piezoresistive sensor for wearable applications and the device fabrication procedure is schematically shown in Figure 8b.[63] Although the progress in 3D printing for functional material engineering, remains challenging especially the resolution. With advances in 3D printing technique, the development of functional composites for future flexible and wearable electronics would advance further.

3.5. Filtration

Filtration has been used to prepare highly uniform composite films for flexible electronics. A porous membrane is used to filtrate the fillers while a positive or negative pressure is applied to control the flow of solvent through the membrane. The fillers and polymer can be dispersed in the organic or aqueous solution for filtration. Composite film with good uniforminity can be realized after filtration because the solvent could be simultaneously extracted from the evenly distributed pores in the filter membranes. Additionally, composite films with different patterns can be obtained by employing filtration mask.[151, 152] Furthermore, the thickness of the composite films can be readily adjusted by varing the concentration of the filler and polymer in the solution. The composite film can be transfered to the template by dissolving the filter membrane or peeling off the composite film from the membrane directly. Yan et al. developed a graphene/nanocellulose composite nanopaper using the filtration technology for strain sensors.[153] The fabrication procedure is schematically illustrated in **Figure 9a** that shows a graphene to nanocellulose weight ratio of 1:1 was suitable for strain sensing application. The composite nanopaper was noticed with excellent flexibility and stretchability as depicted in Figure 9b-e. Additionally, the water droplets on the surface of the crumpled graphene paper

could be absorbed quickly, indicating the formation of porous structures in the nanopaper (Figure 9f). Filtration is a simple and cost-effective approach to fabricate functional composite films and no sofisticated equipment is required. However, filtration technology is time-consuming and the size of the composite film is determined by the size of filtration membrane, which obstruct its compatibility to large-scale production.

3.6. Electrospinning

Electrospinning is a useful and promising approach in the fabrication of continuous, high surface-to-volume ratio polymeric nanofibers.[154, 155] With this technology, polymeric nanofibers can be prepared under an electric field applied between the grounded collector and metal tip of a syringe filled with precursor solution. Recently, ferroelectric polymers such as PVDF and P(VDF-TrFE), have been widely electrospun into nanofibrous mat for energy harvesters.[38, 156, 157] It should be mentioned that the polymer solution can be replaced by the polymeric composite solution to fabricate the functional fibrous composites as well. Lee et al. reported a transparent bending-insensitive tactile sensor based on electrospun CNT/graphene/polymer composite nanofibers.[71] In the fabrication, small quantity of CNTs and graphene were firstly dispersed as conductive fillers in a fluorinated copolymer solution, where the fluorinated copolymer was served as the nanofiber matrix. The functional nanofiber composite was then fabricated by electrospinning. Wang et al. prepared poly(styrene-block-butadiene-block-styrene) (SBS) nanofiber mats via electrospinning technique, followed by drop-casting silver nanoparticles or PEDOT:PSS as the active layer for temperature/pressure bimodal sensors and the fabrication procedure of the sensor is schematically illustrated in **Figure 10a**.[83] As shown by the SEM image in Figure 10b, the AgNPs are closely connected with each other, forming a shell on the surface of the SBS fiber. Recently, MXene has been demonstrated as a promising candidate for flexible electronics. Jiang et al. reported an electrospun MXene/PVA composite matrix as the negative friction layer for TENGs as

depicted in Figure 10c.[158] SEM images in Figure 10d and 10e reveal the morphologies of electrospun PVA and MXene/PVA composite, showing that good networks are formed for both PVA and MXene/PVA nanofibers . Similar to the printing method, the polymer composite can be deposited in large scale via electrospinning, where the thickness and morphology of the polymer composite based nanofibers can be readily tuned by controlling the period of electrospinning. Therefore, electrospinning is a low-cost and simple approach to produce functional polymer nanocomposite based fibers for sensors, batteries and biomedical devices. However, there are some shortcomings for this technique in the fabrication of polymer composite based nanofibers. For example, because of the low concentration of the precursor solution, it is time-consuming to fabricate the composite film in a large scale. Additionally, toxic solvents normally are involved in the preparation of the precursor solution, which threat the human health and environment.

4. Functional Polymer Composite Based Electronics

The advances in functional polymer composites have boosted up the progress of various flexible electronics and integrated systems.[159–164] In this section, representative applications of functional polymer composites for flexible electronics are discussed, with particular focus on flexible strain/pressure sensor, temperature sensor, nanogenerator, and transistor. Meanwhile, the basic sensing mechanisms of representative sensors will be briefly discussed.

4.1. Functional Composite Materials for Strain/Pressure Sensors

Flexible strain/pressure sensors which detect the deformation or pressure stimuli by measuring strain/pressure-induced electrical signals, have obtained broad attentions due to their promising applications in healthcare monitoring, soft robots and artificial intelligence.[165–167] According to their working mechanisms, the strain/pressure sensors are generally divided into four types including piezoresistive, capacitive, piezoelectric and triboelectric sensors.[168–170] The

transduction mechanism of the strain/pressure sensor is the mechanical force induced changes in resistance, capacitance, voltage/current for piezoresistive, capacitive, piezoelectric and triboelectric sensors, which have been detailed in previous works.[171, 172] Compared with the other pressure sensors, piezoresistive sensors have combined merits of simplicity in device fabrication and simple system for signal readout , which make them much more attractive in varities of applications. In this part, we mainly summarize the recent advances of functional polymer composites for flexible piezoresistive strain/pressure sensors.

The performance of flexible strain/pressure sensors is generally evaluated according to the following parameters, such as sensitivity (called gauge factor for strain sensors), response speed, detection range, and durability etc. The gauge factor (*GF*) of the strain sensor is denoted as following:

$$GF = (\Delta R/R_0)/(\Delta l/l_0) \quad (4.1)$$

Where ΔR and R_0 refer to the relative resistance change under strain and initial resistance, respectively. Δl and l_0 are the relative length change under strain and the initial length of strain sensors, respectively. Thus, the *GF* of the strain sensors can be acquired from the plots of relative resistance change to the applied strain.

The sensitivity (*S*) of pressure sensors could be defined as following,

$$S = (\Delta I/I_0)/\Delta P \quad (4.2)$$

where ΔI, I_0 and ΔP refer to relative current change under pressure, current without pressure, and change of applied pressure, respectively. Various materials such as carbon materials, metal nanowires and conductive polymers have been used as conductive fillers in the functional polymer composites for wearable piezoresistive strain/pressure sensors owing to their excellent electrical conductivity and outstanding mechanical properties.[173-176] In the following part,

representative examples of flexible strain and pressure sensors with varieties of functional polymer composites are discussed. The detailed performance of recently reported flexible pressure sensors based on different polymer composite is summarized in **Table 1.**

4.1.1. Functional Composite Materials for Strain Sensors

Strain sensing range and *GF* are two important parameters of flexible strain sensors in valuing the performance of the strain sensors. A wide strain sensing range and high *GF* of the strain sensors are necessary for diverse applications. To achieve strain sensors with a large *GF* over a broad strain range, it is highly desirable to obtain highly stretchable sensing materials. The conventional sensing materials are used by different kinds of methods, including embedding sensing fibers in polymeric matrix[57] or making special structures of the strain sensing layers.[177] However, limited sensitivity or poor stretchability are commonly observed in these sensors, which will limit the application of the strain sensors. To overcome these obstacles, conductive fillers can be filled in the stretchable polymers to produce functional composites with good electrical conductivity, where the strain sensing range and *GF* rely on the properties of the functional composite materials and device fabrication strategies as well.[178] Representative examples of strain sensors with functional composites will be discussed in the following section. For example, a strain sensor based on aligned SWCNTs/ PDMS was reported by Yamada et al. as depicted in **Figure 11a.**[179] When strain forces were applied to the sensor, gaps and islands were simultaneously generated in the CNT film with the islands bridged by interconnected CNT bundles. The strain sensors exhibited excellent properties including a wide sensing range over 280%, a high durability, and a fast response speed. However, the strain sensor exhibited a relatively low GF of 0.82 and 0.06 for 0–40% and 40–200% strain, respectively, which is lower than those of conventional metal film and some other polymer composite based strain sensors.[180] Additionally, although the strain sensor showed good durability over 10, 000 cycles under a strain of 150%, the device performance greatly

decayed after 3, 300 cycles with a strain of 200%. The stretchability of the strain sensor was likely to be enhanced by replacing the PDMS substrate with more stretchable substrates.

In merits of its superior flexibility, good electrical conductivity, and excellent mechanical stability, reduced graphene oxide (rGO) is also an excellent candidate as conducting fillers for polymer composite based wearable strain sensors. For example, a highly sensitive strain sensor based on the rGO/elastomer composite was developed by Tang et al.[181] As schematically illustrated in Figure 11b, the rGO was deposited on a commercially available copper mesh to achieve the rGO microtubes by etching the copper wire in the selected area. According to the unique design, the strain sensor can withstand a stretched strain up to 50% of its original length and show long-time durability over 500 cycles. Additionally, the *GF* of the sensor was up to 630 under an applied strain of 21.3%. This construction can be used to detect human motions such as bending and stretching of human wrist, and recognize vocal speech. However, despite the relatively high *GF* of the rGO composite based strain sensors, the device showed a very low sensing range from 0 to 50%. Thus, it is highly desirable to develop the functional polymer composite based strain sensors with both a high *GF* and broad detection range. Due to their excellent electrical conductivity and mechanical flexibility, AuNWs were employed as the conductive fillers on the elastomeric substrate as strain sensors by Cheng's group.[182] The fabrication of AuNWs strain sensors was carried out by drop-casting the prefabricated AuNWs on the rubber sheets with the assistance of a polyimide mask with a rectangular opening as schematically depicted in Figure 11c. It should be noticed that this is a general route to the fabrication of AuNW film on various rubber substrates such as PET, nitrile rubber, and PDMS with strong adhesion. The ultrathin strain sensors exhibited excellent performance including a wide strain sensing range from 0.01% to 350%, a long-term durability over 5, 000 cycles, a fast response speed of 22 ms, and a gauge factor of 6.9–9.9. The superior device performance allowed the sensors to monitor different human motions such as throat muscle stretching, finger

flexion extension, and human wrist pulses in real time as well. Although AuNW based strain sensors have the wide detection range and high sensitivity, the relatively low production of AuNWs and the high cost of precursor materials obstruct their extensive applications in functional composite polymer based flexible electronics. To reduce the fabrication cost, Zhang's group has developed strain sensors based on the advanced carbon composites.[183] As shown in schematic illustrations in Figure 11d, a strain sensor was prepared with the hierarchically structured carbonized cotton fabric and PDMS composite using a cost-effective and scalable process. The hierarchical structures of the commercial cotton fabrics are critical for achieving strain sensors with high performance. Therefore, the fabric structures could be selected to tune the performance of the strain sensor devices for different applications. The carbonized cotton fabric based strain sensors exhibited superior performance including a large workable strain range over 140%, a gauge factor of 25 and 64 in strain range of 0%–80% and 80%–140%, respectively, and a long-term stability as well. In merits of their fascinating sensing performance, the applications in monitoring human motions including finger bending, wrist pulse, and motions of knee joints were demonstrated, revealing the tremendous potential applications in wearables and artificial intelligence. Zhang's et al., developed high-performance strain sensor using the silk-derived fabric by a low-cost approach. Similarly, the strain sensors developed from the carbonized silk fabric exhibited excellent sensing performance as well.[184]

4.1.2. Functional Polymer Composite Materials for Pressure Sensors

Just as the strain sensors, the flexible pressure sensors have obtained significant research interest because of their potential applications in wearables soft robotics and E-skin.[185, 186] Recently, the conductive functional composites have been widely used as sensing layer for flexible piezoresistive pressure sensors.[187, 188] The sensing mechanisms of the piezoresistive pressure sensor can be summarized as following: i) the applied pressure changes the contact between the functional composites and patterned electrodes. ii) The applied pressure changes the connection between the functional composite layers. iii) The external pressure changes the

bulk conductivity of the functional composite. The applied pressure can change the electrical signals of pressure sensor devices, which accordingly achieve the detection of the external pressures. For example, an ultrasensitive and fast response pressure sensor with a rGO/PVDF nanofiber composite was developed by Lou et al, where the PVDF nanofibers were prepared by electrospinning.[189] As schematically depicted in **Figure 12a**, the rGO wrapped PVDF nanofiber composites were fabricated by a simple solution process. With the rGO/PVDF composite as the pressure sensing layer, the device was constructed as depicted in Figure 12a. As observed from the SEM image, the PVDF nanofibers showed high aspect ratios, enabling the composite film with excellent flexibility. The sensing mechanism of the pressure sensor device is based on the external pressure between the composite films and the copper electrodes. According to the excellent properties of the rGO/PVDF composite, the developed pressure sensors showed fascinating performance including a linear sensitivity of 15.6 kPa^{-1} in the sensing range of 20—60 kPa, a LOD of 1.2 Pa, a fast recovery time of 7 ms, and excellent long-term durability more than 100,000 cycles. In terms of applications, the pressure sensors were employed to detect the muscle movement, physiological signals and spatial pressure distribution as E-skin by integrating the devices into sensor arrays.

Inspired by the microstructures of human skin epidermis, a hierarchically structured GO/PDMS composite film was developed by Ren et.al. as pressure sensors.[34] For the fabrication of functional composite film, a sandpaper template was employed to obtain the surface microstructures. Additionally, pressure distribution for various geometries including pyramid, hemisphere, nanowire, and random distribution spinosum (RDS) microstructures were simulated as depicted in Figure 12b. The pressure sensor with RDS microstructures was simulated with much higher sensitivity than the other microstructures based sensors. The RDS microstructure based pressure sensor exhibited a pressure sensitivity and a linearity range of 25.1 kPa^{-1} and 0–2.6 kPa, respectively. According to the sensing mechanism and simulation analysis, the high sensitivity and linearity range were attributed to the spinosum microstructure

and random distribution on the surface of composite film, respectively.

Inspired by the hierarchical microstructures of biological systems from nature, Ha et al. developed a highly-sensitive and fast-responsive E-skin with an interlocked geometry of hierarchical PDMS/ZnO micropillars as shown in Figure 12c.[30] With the unique design, the flexible piezoresistive sensor exhibited a high pressure sensitivity of 6.8 kPa^{-1} a low detection limit of 0.6 Pa, and a fast response speed (< 5 ms).

To expand the application of wearable pressure sensors, high sensitivity over a wide pressure sensing range is desired. In our recent work, we developed a fingertip skin-inspired piezoresistive sensor employing the conductive graphite/PDMS as the sensing layer.[66] The graphite/PDMS composite film possessed hierarchical microstructures on its surface and porous microstructures inside the composite, mimicking the microstructures of human fingertip skin. Two layers of composite films were face-to-face laminated to fabricate the piezoresistive pressure sensor with the ITO/PET as bottom and top electrodes. Because of the hierarchical microstructures on the surface of the active films, the piezoresistive pressure sensor realized an ultrahigh sensitivity and a wide detection range due to the porous structures. Notably, the surface microstructures were duplicated from the commercially available sandpaper which was widely used in achieving the microstructures in material engineering, and the sponge structures were prepared by employing NaCl sacrifice template. It should be noticed that there were no expensive materials or sophisticated equipment were utilized in the entire fabrication process of the hierarchically microstructured graphite/PDMS films. Our fingertip skin-inspired device showed a high sensitivity of 245 kPa^{-1} over a wide linear pressure range from 5 Pa to 120 kPa and a response time of 4 ms. The pressure sensor was demonstrated to distinguish different forces such as pressing, bending, and twisting. Furthermore, by employing the hierarchically structured PDMS as the substrate, the pressure sensor could efficiently detect the surface texture of the objects as human fingertip skin (Figure 12d). The skin sensors were further demonstrated with the application in monitoring artery wrist pulses in rest state and after

exercises, detecting the wrist bending states, and controlling the grasping force of a robotic arm.

4.3. Functional Polymer Composite for Temperature Sensors

Obtaining the actual or relative temperature is critical for various applications, so the temperature is one of the most commonly sensed stimuli in nature and human bodies. In particular, human body temperature plays an important role in detecting human activities and underlying the health condition of human body. To detect the temperature of human body and to develop E-skin, various flexible and wearable temperature sensors have been proposed in the past decades. According to the sensing mechanisms, the temperature sensors are basically divided into the following types: transistor-based, thermoelectric-based and thermistor-based temperature sensors.[190–193] Among them, thermistor-based temperature sensors have obtained much more attentions because of their simple device construction, low fabrication cost and easy-signal processing. In this part, we mainly review the recent advances in functional polymer composite based thermistor temperature sensors. The device fabrication and working mechanisms of other types of temperature sensors can be found in the literature.[193] The detection resolution and sensitivity are two critical parameters to assess the performance of the temperature sensors. In general, the sensitivity of a thermistor can be assessed by the temperature coefficient of resistance (α) with the following equation:

$$\alpha = (\Delta R/R_0)/\Delta T \qquad (4.3)$$

Where ΔR, R_0, and ΔT are the resistance change, initial resistance, and change in temperature of the temperature sensor, respectively.

Due to their excellent flexibility, various polymer composites have been applied in the development of high performance wearable thermistors.[194, 195] For instance, Kim et al. reported a temperature sensor with high sensitivity and good detection resolution using functional AgNPs/polymer composite.[196] In the device fabrication, a long and bent organic

conductor/elastomer/AgNPs composite (PEDOT:PSS/PUD/AgNP) line was obtained as the temperature sensing layer by inkjet printing (**Figure 13a**). As depicted in Figure 13a, it was observed that the temperature sensor exhibited a sensitivity of 0.32% per °C, negligible heating and cooling hysteresis, and a temperature detection resolution of 0.5 °C. Additionally, there was almost no decay in electrical characteristics even after 5000 bending cycles, indicating excellent mechanical stability. Furthermore, a temperature sensor array was demonstrated to detect the temperature in real time, revealing the potential application as E-skin for robots. In another example, a flexible ferroelectric composite film was fabricated by introducing GO sheets into a PVDF matrix followed by rod casting under a temperature of 50 °C for 12 hours (Figure 13b).[31] The rGO/PVDF composite based temperature sensor showed a wide temperature detecting range (0–100 ^{o}C). The rGO/PVDF composites with various rGO contents were prepared and the relative resistance ($\Delta R/R_0$) was plotted as a function of temperature for all composite films. It was interestingly found a negative temperature coefficient (NTC) of resistance, which is not common for conductive composites. This phenomenon was attributed to the enhanced contact between rGO sheets with increasing temperature and intrinsic NTC behavior of rGO. Flexible temperature E-skin was developed by placing gold electrodes arrays on the bottom and top of the rGO/PVDF composite film (Figure 13b). As shown in Figure 13b, the temperature variation over the contact area was well revealed by the temperature sensor array when human hand was placed on top of the E-skin. The real-time temperature monitoring of human skin can provide useful information for clinical diagnosis.

Flexible and wearable temperature sensing E-skins are highly desired so as to be readily attached onto human skin to minimize the environmental influence for more accurate detection. For example, functional composite films of pNIPAM/PEDOT:PSS/CNT and bio-inspired PDMS/pNIPAM were prepared by Oh et al. in developing ultra-flexible and wearable sensors for human body temperature monitoring.[197] As exhibited in Figure 13c, the E-skin with good

flexibility can be well attached on human skin and the schematic diagram of the device structure is shown in the right part of Figure 13c. The octopus's sucker inspired microstructures allowed the temperature sensor to realize a strong attachment with human skin. Furthermore, the temperature E-skin showed a sensitivity of 2.6%·°C^{-1} between 25 and 40 °C, so a small temperature change of 0.5 °C in human skin can be accurately detected.

4.4. Functional Polymer Composites for Energy Harvesters

Nanogenerator, a promising energy harvester for scavenging and converting mechanical energy into electrical power, has obtained worldwide research interest because of its promising application in wearable electronics and energy charging systems.[198–200] Recently, various nanomaterials including ZnO NWs, $BaTiO_3$ NPs, and Ag NWs have been employed as the fillers in polymers to obtain functional composites for piezoelectric and triboelectric nanogenerators.[201–203] For piezoelectric nanogenerators, the output performance of the energy harvester can be enhanced by introducing piezoelectric nanomaterial fillers into the polymer. For example, Lee et al. reported a functional composite film composed of amine-functionalized lead zirconate titanate (PZT) nanoparticles (PZT-NH2 NPs) and a thermoplastic polymer for piezoelectric nanogenerators (PNGs).[204] It was proved by the authors that piezoelectric properties of the nanomaterials and their uniform dispersion in the polymer matrix were critical to achieve high-performance piezoelectric nanogenerators. The PZT-NH_2/polymer composite based flexible PNG devices achieved an open-circuit voltage (V_{OC}) of 65 V and short-circuit current (I_{SC}) of 1.6 mA during bending/unbending cycles. Furthermore, the power generated by a PNG device was demonstrated to be sufficient enough to power a commercial LED without any storage modules. Additionally, the PNG device could be combined with a capacitor to build a power module for self-powered systems. Triboelectric nanogenerators (TENGs), another widely studied energy harvester, have obtained significant attentions for self-powered and wearable electronic devices thanks to their simple fabrication, low fabrication cost, high

output power density, and excellent mechanical properties. Similarly, functional polymer composites have been widely employed as triboelectric layers for TENGs.[205, 206] For example, Fan and co-authors reported a stretchable TENG with porous CNTs/PDMS composite as depicted in the schematic diagram of the device fabrication (**Figure 14a**).[207] The effect of the CNTs content on the output voltage is shown in the right part of Figure 14c. It was observed that the TENG device showed the highest output voltage with a CNT percentage of 15% and the further addition of CNTs was demonstrated with negative effect on the device performance. A highly conductive ferroelectric cellulose composite was developed by Oh et al. for TENGs and the schematic fabrication of the BC composite paper is shown in Figure 14b.[208] The cellulose-based composite paper was simply fabricated by vacuum filtration of a mixed suspension comprising BC fibers, AgNWs, and BTO NPs, which was followed by drying and hot pressing processes. The SEM images of the BC composite paper revealed the existance of AgNWs and BTO NPs in the composite. Based on the composite film, the TENG exhibited a maximum V_{OC} of 460 V and a I_{SC} of 23 μA, respectively (Figure 14b). As a power-supply unit, the TENG driven by repeated hand tapping could directly power 200 commercial LEDs without energy storage modules.

4.5. Advanced Composite for Bimodal Sensors

Human skin has the capability to simultaneously detect different stimuli, such as humidity, temperature, touch, and friction. Therefore, it is significant to develop skin-like sensors with multifunctional sensing abilities for diverse applications. In this section, we discuss the temperature/pressure bimodal sensors based on the functional polymer composites.

Bae et al. achieved a pressure/temperature bimodal E-skin with linear sensitivity and stimulus discriminability by employing the SWNT/PDMS composite with surface-wrinkled pyramidal microstructures as the pressure sensing layer and planar rGO film as the temperature sensing layer, respectively.[190] The schematic illustration of the bimodal E-skin using a layer-by-layer

structure is shown in **Figure 15a**. Based on the bimodal sensor, pressure and temperature can be simultaneously detected and categorized in real time. The sensing mechanism of the bimodal sensor is the temperature dependent resistance change of the rGO film and the pressure dependent contact area between the dielectric layer and electrode. Based on the single bimodal sensor, they developed a flexible 4 × 4 bimodal sensor array to detect the spatial pressure distribution and temperature in real time. As depicted in the bottom of Figure 15a, the sensor array could detect the temperature and pressure distribution of the bottles simultaneously. Zhang and co-authors reported a flexible and self-powered temperature/pressure dual-parameter sensor array with PEDOT:PSS/PU composite film.[209] The bimodal sensor exhibited a pressure sensitivity of 20 kPa^{-1} and a high resolution of 0.1 K in detecting temperature. The developed bimodal sensor arrays were able to detect the spatial pressure and temperature distribution with high resolution as depicted in Figure 15b. The bimodal sensor arrays showed potential applications in wearable electronics and E-skin. As shown in Figure 15c, based on the silk-nanofiber-derived carbon fiber membranes (SilkCFM), Zhang's group reported a temperature/pressure bimodal sensor by assembling a temperature and strain sensor.[184] The strain sensor showed an extremely high *GF* of 8350 at 50% strain, allowing the sensor to detect tiny strain induced by the pressure stimuli. Additionally, the temperature sensor showed a high resolution of 1 ^{o}C over a wide temperature range from 35 to 80 ^{o}C. A bimodal sensor array was developed to detect the pressure and temperature distribution as well, demonstrating the promising potential as E-skin for robots.

Apart from the above mentioned carbon based materials, metal−organic frameworks (MOFs), a class of crystalline materials assembled by metal ions as the nodes and organic ligands as struts, have obtained worldwide research attentions in sensors.[210–212] Zhao et al. reported a MOF-derived carbon/PDMS composite for temperature/pressure bimodal sensors as depicted in Figure 15d.[213] The as developed sensors exhibited a high pressure sensitivity of 15.63 kPa^{-1}

and a temperature sensitivity of 0.11 $^{o}C^{-1}$ as depicted in Figure 15d. The above results have demonstrated that the functional polymer composites are excellent candidates for bimodal sensors. The functional polymer composites fabricated with cost-effective and large-scale compatible approaches are more promising for future bimodal sensors.

4. 6. Functional Polymer Composites for Transistors

4.6.1. Polymer Composite Based Gate Dielectrics

FETs are the basic building blocks for electronic circuits and sensors, where the device structures and underlying mechanism of which have been detailed introduced in previous review papers.[214, 215] Gate dielectric is one of the critical components in the construction of FETs, which can control the conduction channel thereby the drain current between source and drain electrodes. The drain current of the transistors could be expressed as following:

Linear regime,

$$I_{lin} = \frac{W}{L}\mu_{FE}C_i(V_{GS} - V_T - \frac{V_{DS}}{2})V_{DS} \qquad V_{DS} << V_{GS}\text{-}V_T \qquad (4.4)$$

Saturation regime,

$$I_{sat} = \frac{W}{2L}\mu_{FE}C_i(V_{GS} - V_T)^2 \qquad V_{DS} \geq V_{GS}\text{-}V_T \qquad (4.5)$$

where W, L, μ_{FE}, and C_i represent the channel width, channel length, carrier mobility, and unit capacitance, respectively. V_T is the threshold voltage, and V_{DS} is the drain to source voltage, respectively. Because the performance of FETs is closely related to the properties of the gate dielectrics, great efforts have been devoted to the development of high dielectric films for achieving low-power FETs. Particularly, due to their intrinsically high dielectric constant, the inorganic dielectrics including Al_2O_3, HfO_2, ZrO_2, etc. are widely used as dielectrics for low-power FETs.[216–218] However, cracks usually occur when the metal oxide dielectrics are under

mechanical bending, which limits their application for flexible FETs. On the other hand, the polymer dielectrics have the property of excellent flexibility for flexible FETs, but the dielectric constants of the polymer dielectric layers are usually low, obstructing their applications for low-power FETs. Alternatively, the inorganic nanoparticle/polymer nanocomposites have the high dielectric constant as the inorganic materials and maintain the flexible property of the polymer, which makes them excellent candidates for low-power flexible FETs and related sensors. Zirkl et al. demonstrated a high-*k* gate dielectric based on metal oxide/polymer functional nanocomposite for low-voltage flexible OFETs and sensors (**Figure 16a**).[219] As revealed in the AFM image, the ZrO_2/poly(a-methyl styrene) (PaMS) nanocomposite gate dielectric layer showed smooth surface with a rms-roughness of 0.4 nm compared with that of the bare ZrO_2 gate dielectric layer. With inorganic/polymer nanocomposite dielectric layer, the OFET device exhibited a high areal capacitance of 150 nF/cm^2, a carrier mobility of 0.9~1.2 cm^2 V^{-1} s^{-1}, current on/off ratio of 10^6, subthreshold swing (SS) of 110 mV dec^{-1} and a low operation gate voltage of -1.5 V. The results demonstrated that ZrO_2/PaMS functional nanocomposite is an excellent candidate for high-performance OFETs. In addition, they demonstrated ZrO_2/PaMS nanocomposite based OFETs on the flexible PET substrate as low-power driven sensors. As an another example, Hur et al. reported a stretchable polymer/hafnium oxide (HfO_2) composite gate dielectric layer prepared at low temperature for high-performance flexible indium gallium tin oxide (IGTO) FETs (Figure 16b).[220] The composite dielectric layer was composed of PVP-co-PMMA and HfO_2 with various ratios. The relative dielectric constants (*k*) and breakdown electrical field (E-field) for various dielectric films with different nanocomposite compositions were investigated, reflecting the loading effect of high-*k* HfO_2 in the polymer matrix. With the optimized gate dielectric, a lowest leakage current of 5.8×10^{-9} A/cm^2 and highest breakdown electric field of 3.8 MV/cm were achieved for the FET, demonstrating an excellent insulating property of the polymer composite. The transfer characteristics of various nanocomposite gate dielectrics based IGTO transistors

are shown at the bottom of Figure 16b. The device based on a control dielectric layer (H0) showed a reasonable carrier mobility of 12.8 cm^2 V^{-1} s^{-1}, which is attributed to the efficient percolation pathways for electrons in IGTO active layer. However, the device based on H0 gate dielectric exhibited a large SS of 2.8 V/decade, a negative and a high off current of 1×10^{-9} A, which was caused by the energetic ion bombardment effect. The transistors based on the UV-treated H50 gate dielectric layer showed significant improvement in mobility, SS, and threshold voltage compared with the devices based on the H0 gate dielectric layer. Additionally, the transistors based on the UV-treated composite gate dielectric showed a high current on/off ratio of 10^7 because of the reduction in off current. Considering the performance of the devices based on different dielectrics, the electrical stability of the IGTO FETs with H50UV composite dielectric under bending stress was studied by fabricating on a flexible substrate via a transfer method as depicted in Figure 16b. The recession of switching capability was negligible even after 100 bending cycles with an extremely small bending radius of 1 mm, which was attributed to the excellent bendability and stretchability of the functional composite dielectric layer. The results reported in this work demonstrated the feasibility of functional polymer/inorganic composite as gate dielectric layers for high performance flexible electronics.

4.6.2. Functional Polymer Composite Based Electrodes and Semiconductors

Intrinsically stretchable semiconductors with high mobility are critical to achieve highly stretchable electronics and sensors for many applications in which huge mechanical deformation is involved.[221, 222] Recently, Sim et al. reported stretchable transistors based on a high mobility semiconductor by importing the metallic CNTs into the polymer semiconductor to obtain the functional composite semiconductor.[223] In this work, the transistors and related arrays were all developed from the stretchable composite materials, comprising the metallic CNTs doped P3HT-NFs/PDMS composite as a semiconductor and AuNPs-AgNWs embedded in PDMS matrix (AuNPs-AgNWs/PDMS) as electrodes. The optical microscopy image of the

stretchable transistor is shown in **Figure 17a** with m-CNT–doped P3HT-NFs/PDMS composite as the semiconductor, AuNPs-AgNWs/PDMS as the source and drain electrodes, and the ion gel as the gate dielectric layer. The configuration of the stretchable transistor and its charge transport are schematically depicted in Figure 17a. It was demonstrated that the mobility of the semiconductor was improved by doping the metallic CNTs due to its enhanced electrical conductivity. Meanwhile, effects of the doping concentration were investigated in this work which revealed that the mobility of the semiconductor increased while the current on/off ratio decreased when increasing the ratio of the metallic CNTs in the functional composite. The increased carrier mobility was attributed to the shortened transport distance in the conduction channel, leading to a higher effective carrier mobility. Furthermore, fully stretchable 8 × 8 transistor array was fabricated based on a solution process to illustrate its potential application for high-performance integrated stretchable electronics. The optical microscopy image of the transistor array is shown in Figure 17a. Various mechanical deformation containing poking, stretching and crumpling were performed without any physical damages. When the transistor was stretched up to 150% of its original length along the channel length direction, a moderate decrease in carrier mobility and a slight shift in V_T are observed. After the mechanical stress was fully released, the carrier mobility and V_T recovered to almost 70% and 97% of its original values. When the device was stretched by up to 150% of its original length perpendicular to the channel length direction, decrease in mobility and a slight change in V_T were clearly observed. Similarly, after the release of the strain, the mobility and threshold voltage recovered 52% and 92% of its original values, respectively. Finally, the tactile sensors based on the stretchable transistor arrays for elastic E-skin were demonstrated. This work proved the applications of functional composite semiconductors in stretchable electronics.

Recently, Bao et al. have reported a stretchable and self-healing semiconductor by blending the illustrating elastomer and polymer semiconductor through dynamic cross-linking as transistors

and strain sensor array.[224] The functional composite semiconductor was demonstrated with an excellent stretchability up to 1500% of its original length and a good self-healing ability at room temperature. The strain sensor based on the stretchable semiconductor exhibited an ultrahigh gauge factor of 5.75×10^5, further demonstrating the potentials of functional polymer composites as stretchable transistors and sensors.

5. Functional Composite Material Based Sensors for Health Monitoring and Aftificial intelligence

In this section, we present the representative applications of the functional composite based sensors for health monitoring and artificial intelligence.

5.1. Functional Composite Material Based Sensors for Health Monitoring

The functional composite material based sensors (strain, pressure, and temperature sensors) have been broadly employed in health monitoring according to their merits of excellent flexibility and the ability to collect the physiological signals in real time. The sensors have showed great potentials in monitoring human body temperature, collecting real-time wrist pulse signals, voice recognition, and mapping plantar pressure distribution, which can provide important information in diagnosis and treatment for patients.

5.1.1. Wrist Pulse and Blood Pressure

In the past a few years, because the wrist pulse waveform can provide useful information for medical diagnosis, tremendous efforts have been dedicated to the development of the strain/pressure sensors with the capability of obtaining high-resolution wrist signals. Especially, the piezoresistive pressure sensors have appealed more attentions because of their easy signal processing and simple device structures. Conductive composite films with microstructures (regular or irregular microstructures) are used as the pressure sensitive layers in the device

because the microstructure can enhance the sensitivity of the sensor in detecting tiny pressure from the wrist pulses.[21, 65] Choong et al. reported a stretchable piezoresistive pressure sensors with regularly patterned conductive PEDOT:PSS/PUD composite for wrist pulse detection. The piezoresistive pressure sensor was attached onto the radial artery and high signal-to-noise pulse waveform was obtained as depicted in **Figure 18a**. As shown in the enlarged view of one pulse waveform (Figure 18a), two identical peaks (systolic and diastolic) were obtained and the blood pressure (BP) was estimated at the same time. A "pulse pressure" of 1.3 mmHg was obtained, which was much lower than the actual blood pressure~40 mmHg.[33] However, for practical applications, the absolute value of BP is critical and highly desired. To obtain BP and wrist pulses, Luo et al. developed a piezoresistive pressure sensor with a hollow-structured graphene/silicon composite.[225] In this work, sensor was placed on human wrist to record wrist pulse signals and the collected signals are depicted in Figure 18b. Additionally, the reference wrist pulse signals were collected by a commercially available BP monitoring machine (Finometer). The wrist pulse signals measured by the pressure sensor was correlated with the systolic blood pressure (SBP), diastolic blood pressure (DBP), and mean blood pressure (MBP) obtained from the Finometer. This work successfully demonstrates that the functional polymer composite based pressure sensor has potential application as a cuffless BP measurement or calibration unit in future.

5.1.2. Voice Recognition

Speaking is the most direct way of communication among human beings, where the sound is generated through the vibration of vocal folds during the speaking process. The pressure changes across the larynx can bring the gentle movement of throat accompanying by phonation. Tracking the tiny movement of the throat is an effective way to record the speaking. Particularly, it is meaningful for people with difficulties in voicing and tracking the muscle movement over the throat can reveal the speech. Therefore, the ultrasensitive pressure/strain

sensors are highly desired to detect the tiny muscle movement. Significant efforts have been dedicated to the development of highly sensitive sensors for voice recognition in the past years. The conductive composite films with microstructures have been demonstrated as one of the most effective candidate as active layers for pressure sensors in voice recognition. Our group developed a graphite/PDMS composite film with hierarchical microstructures developed from commercially available sandpaper template. The sensor was fixed on the throat of a volunteer as presented in **Figure 19a**.[65] Different signal patterns were obtained when the volunteer spoke "Hello", "Nature", and "Pressure Sensor", indicating the capability of the functional composite based pressure sensor for voice recognition. Additionally, when the volunteer repeated the same word for three times, almost identical patterns were obtained, proving the reliability for voice recognition. Moreover, Wu et al. developed a pressure sensing platform employing the CB/PU sponge for voice recognition and highly repeatable current patterns were obtained for different words. Additionally, all materials used in the study were inexpensive, proving a feasible way for the mass production of pressure sensors.[60]

5.1.3. Plantar Pressure Distribution Mapping

Mapping the plantar pressure distribution is regarded as one of the significant strategies in shoe design and some other healthcare monitoring systems. Particularly, unbalanced foot pressure distribution and abnormal gait patterns may induce serious feet diseases. Additionally, it is reported that there is a representative gait pattern for patients with Parkinson's disease.[226] Therefore, it is meaningful to study the plantar pressure distribution in the aspects of disease prediction, diagnosis, and monitoring. A high pressure sensitivity in the low pressure range is required for the wrist pulse detection due to the tiny pressure change induced by the wrist pulses. However, for the plantar pressure distribution mapping, a high sensitivity over a broad pressure range is required because of the large pressure applied on the sensor by body weight. The conductive composite films with microstructures are the excellent candidates for pressure

sensors persuing high sensitivity over broad pressure range. Lee et al. reported multilayer E-skin with great potential for plantar pressure distribution mapping.[6] The schematic diagram of the sensor array is presented in Figure 19b, including the supporting PET film, patterned electrodes, and multilayered E-skins. To check the capability of the pressure sensor arrays in pressure distribution mapping, a petri dish was put on top of the pressure sensor array and the pressure distribution was readily revealed. Moreover, a smart insole made up of E-skins was reported that detected the foot pressure distribution during walking. As shown at the bottom of Figure 19b, the smart insole precisely detected the foot pressure distribution, demonstrating its potential applications in sports industry and wearable medical electronics.

5.2. Functional Composite Material Based Sensors for Artificial Intelligence

Strain/pressure sensors are proved with the great potential in building smart human-machine interfaces.[39, 227] The signals collected by the strain/pressure sensors can be used to control smart robots. Therefore, different kinds of smart gloves were developed based on wearable, stretchable and skin-mountable strain sensors for the bending angle measurement of finger joints.[228, 229] Someya's group reported the printable conductive AgNPs/rubber composite based strain sensors for application in smart gloves, where the AgNPs were developed by the in situ, solely by mixing Ag flakes, surfactant and fluorine rubbers.[230] Their printable elastic composites exhibited conductivity higher than 4,000 S cm^{-1} and 935 S cm^{-1} at 0% strain and when it was stretched up to 400%, respectively, indicating an excellent conductive property for flexible and stretchable electronics. The composite was printed on textiles for temperature or pressure sensors. The test results showed that the sensors were still stretchable and functional even after 120% strain, and the stretchability was limited by the property of the textile. The sensors could be easily placed on human and robot as wearables. Furthermore, pressure sensor arrays with high spatial resolution are desired for robot as electronic skin. A nature inspired sensory system was developed by Kang et al. by mimicking the sensory system of the spider,

which is ultra-sensitive to strain and vibration.[231] To demonstrate the device's scalability and ability to detect mechanical vibrations and pressure, a 8 × 8 pixel array was developed by them. The static pressure loaded by the PDMS and the dynamic pressure loaded by the flapping ladybird were well revealed by the sensor arrays, demonstrating its application in detecting both dynamic and static pressures.

As is known by us that the distributed network composed of neurons, receptors and synapses in the somatosensory system can process the complex tactile information, which is meaningful for human being and animals (**Figure 20a**).[232] It is equally important to build the artificial somatosensory network system for the smart robots in the future. Kim et al. recently have developed a bio-inspired flexible organic artificial afferent nerve integrated by a pressure sensor array, ring oscillators, and a synaptic transistor as shown at the bottom of Figure 20b. In the system, the tactile information collected by the pressure sensor array was converted as action potentials by the ring oscillators and the action potential was then integrated with a synaptic transistor. The bio-inspired sensory system was demonstrated with the capability to distinguish braille characters and detect the movement of an object. Furthermore, the artificial afferent nerve was connected to motor nerves to build a bio-electronic reflex arc to actuate muscles, proving a significant potential of the bio-inspired sensory system for future artificial intelligence.

6. Conclusion and Perspectives

In the present review, we have summarized the recent developments in the rational design and controlled preparation of functional polymer composites towards flexible and wearable electronic applications. Various conductive/nonconductive fillers, such as carbon-based nanomaterials, metallic nanomaterials, polymers, and metal oxide nanomaterials, have been incorporated into polymer matrix to develop functional polymer composites with desired

properties. Depending on the electrical conductivity, the functional polymer composites are classified into conducting, semiconducting, and insulating functional polymer composite, and various applications in flexible electronics such as strain/pressure sensor, temperature sensor, energy harvester, and transistor have been demonstrated successfully.

Depending on the requirements of different flexible electronic components and sensors, the fillers with controlled micro-/nanostructures have been conceived to enhance the electrical and mechanical properties of functional composites, thus leading to successful implementation in diverse practical applications. As conductive electrodes for the flexible/stretchable electronics, 1D filler materials, such as CNTs AuNWs, and AgNWs, have exhibited promising potential in terms of facilitating an electrically conducting percolation network in extreme conditions. However, although significant progress has been made in developing conductive polymer composites, several challenges still remain in such functional polymer composites. In consideration of processibility, long metallic NWs, which are broadly employed as the conductive fillers for stretchable conductors, tend to precipitate gradually in solution because of their large weight and dimensions. To obtain a homogeneous dispersion of these NWs without sacrificing the high aspect ratios is highly desirable for high performance devices based on solution-processed fabrication route, but it is practically difficult. On the other hand, CNTs show a reduced conductivity in comparison with metallic nanowires, despite their high strength, scalability and surface area to volume ratio.

Environmental stability of the 1D metallic NWs is another issue should be addressed in the future. Although many reported functional polymer conductors containing AgNWs likely to work well in a short time, they may be susceptible to oxidation and the performance of the device will be deteriorated over time generally owing to the increased contact resistance between the AgNWs. AuNWs are excellent alternative to the AgNWs because of their high flexibility, good tolerance to oxidation. Moreover, AuNWs are superior to AgNWs in

consideration of long-time toxicity and biocompatibility. However, the AuNWs are suffering from the relative low yield and high fabrication cost, which limit their large-scale applications for flexible electronics. Alternatively, developing the Ag-Au core-shell structured fillers may overcome the above mentioned limitations of both Ag and AuNWs, wherein the Ag core retains the good electrical properties and the Au shell enhances the biocompatibility and anti-oxidation properties.

As a conductive active sensing layer for the flexible/stretchable sensors, the structural and rational design of the functional polymer composites can enhance the flexibility and sensitivity of the sensors. The microstructured design of the sensing element has been employed as an effective strategy to enhance the sensitivity of pressure sensors. In view of the development of the flexible electronics and related sensors over the past decades, the main challenges for future development of functional polymer composite based flexible electronics and sensors are summarized as following:

i) Strategies for large-scale and cost-effective production of functional nanomaterials with desired morphologies and microstructures, and approaches for reproducible construction of polymer composites for flexible sensors.

ii) Self-healable polymer composites with self-healing ability similar with that of human skin are still highly required for the functional polymer composite based E-skin.

iii) Integration of multiple sensing functionalities of the polymer composite based sensors and power supply on a single technology platform.

iv) The development of technologies that can facilely integrate wearable sensors with other functional parts for a whole wearable smart system.

With the development of polymers, nanomaterial fillers, device manufacturing technologies and engineering technologies, functional polymer composites would innovative next-generation flexible and stretchable electronics**.**

Acknowledgements

The authors acknowledge the grant from the National Natural Science Foundation of China (Grant No.51702055, 62073084, 11904056, and 11704079), the Basic and Applied Basic Research Fund of Guangdong (Grant No. 502220023) and the Basic and Applied Basic Research Fund of Guangzhou (Grant No. 202201010614).

Received: ((will be filled in by the editorial staff))
Revised: ((will be filled in by the editorial staff))
Published online: ((will be filled in by the editorial staff))

References

[1] S. Choi, S. I. Han, D. Jung, H. J. Hwang, C. Lim, S. Bae, O. K. Park, C. M. Tschabrunn, M. Lee, S. Y. Bae, J. W. Yu, J. H. Ryu, S. W. Lee, K. Park, P. M. Kang, W. B. Lee, R. Nezafat, T. Hyeon, D. H. Kim, *Nat. Nanotechnol.* **2018**, *13*, 1048.

[2] S. T. Han, H. Peng, Q. Sun, S. Venkatesh, K. S. Chung, S. C. Lau, Y. Zhou, V. A. L. Roy, *Adv. Mater.* **2017**, *29*, 1700375.

[3] M. Li, S. Chen, B. Fan, B. Wu, X. Guo, *Adv. Funct. Mater.* **2020**, 2003214.

[4] Y. Wang, Y. Yu, J. Guo, Z. Zhang, X. Zhang, Y. Zhao, *Adv. Funct. Mater.* **2020**, 2000151.

[5] K. Meng, X. Xiao, W. Wei, G. Chen, A. Nashalian, S. Shen, X. Xiao, J. Chen, *Adv. Mater.* **2022,** *34*, 2109357.

[6] Y. Zhou, L. Zhao, W. Tao, T. Wang, P. Sun, F. Liu, X. Yan, G. Lu, *ACS Appl. Mater. Interfaces* **2022**, *14*, 19949..

[7] C. Wu, T. Kim, J. Park, B. Koo, S. Sung, J. Shao, C. Zhang, Z. L. Wang, *ACS Nano* **2020**, *14*, 1390.

[8] X. Qu, J. Xue, Y. Liu, W. Rao, Z. Liu, Z. Li, *Nano Energy* **2022**, *98*, 107324.

[9] Y. Li, Y. Cui, M. Zhang, X. Li, R. Li, W. Si, Q. Sun, L. Yu, C. Huang, *Nano Lett.* **2022**, *22*, 2817.

[10] Y. Wu, Y. L, Y. Zhou, Q. Man, C. Hu, W.Asghar, F. Li, Z. Yu, J. Shang, G. Liu, M. Liao, R. -W. Li, *Sci. Robot.* **2018**, *3*, eaat0429.

[11] M. Yang, Y. Cheng, Y. Yue, Y. Chen, H. Gao, L. Li, B. Cai, W. Liu, Z. Wang, H. Guo, N. Liu,Y. Gao, *Adv. Sci.* **2022**, *9*, 2200507.

[12] T. H. Chang, Y. Tian, C. Li, X. Gu, K. Li, H. Yang, P. Sanghani, C. M. Lim, H. Ren, P. Y. Chen, *ACS Appl. Mater. Interfaces* **2019**, *11*, 10226.

[13] L. Lo, J. Zhao, H. Wan, Y. Wang, S. Chakrabartty, C. Wang, *ACS Appl. Mater. Interfaces* **2022,** *14*, 9570-9578.

[14] G. Gou, X. Li, J. Jian, H. Tian, F. Wu, J. Ren, X. Geng, J. Xu, Y. Qiao, Z. Yan, G. Dun, C. Ahn, Y. Yang, T. L. Ren, *Sci. Adv.* **2022** *8*, eabn2156.

[15] F. Wang, J. Chen, X. Cui, X. Liu, X. Chang, Y. Zhu, *ACS Appl. Mater. Interfaces* **2022**, *14*, 26, 30268.

[16] T. Zhu, K. Wu, Y. Xia, C. Yang, J. Chen, Y. Wang, J. Zhang, X. Pu, G. Liu, J. Sun, *Nano Lett.* **2022**, *22*, 16, 6637.

[17] J. He, R. Zhou, Y. Zhang, W. Gao, T. Chen, W. Mai, C. Pan, *Adv. Funct. Mater.* **2022** *32*, 2107281.

[18] J. Shin, B. Jeong, J. Kim, V. B. Nam, Y. Yoon, J. Jung, S. Hong, H. Lee, H. Eom, J. Yeo, J. Choi, D. Lee, S. H. Ko, *Adv. Mater.* **2020**, *32*, 1905527.

[19] Y. Lu, J. Wang, J. He, L. Zou, D. Zhao, S. Song, *ACS Appl. Mater. Interfaces* **2022**, *14*, 29250.

[20] S. Xia, Y. Long, Z. Huang, Y. Zi, L. Tao, C. Li, H. Sun, J. Li, *Nano Energy* **2022**, *96*, 107099.

[21] Q. J. Sun, X. H. Zhao, C. C. Yeung, Q. Tian, K. W. Kong, W. Wu, S. Venkatesh, W. J. Li, V. A. L. Roy, *ACS Appl. Mater. Interfaces* **2020**, *12*, 37239.

[22] C. Wu, T. W. Kim, J. H. Park, B. Koo, S. Sung, J. Shao, C. Zhang, Z. L. Wang, *ACS Nano* **2020**, *14*, 1390.

[23] T. Ye, Q. Wang, C. Tian, R. Singh, Y. Zhang, Z. Liu, X. Fang, D. He, *Adv. Electron. Mater.* **2020**, *6*, 1901291.

[24] S. Choi, S. I. Han, D. Kim, T. Hyeon, D. H. Kim, *Chem. Soc. Rev.* **2019**, *48*, 1566.

[25] M. Xie, Y. Zhang, M. J. Krasny, C. Bowen, H. Khanbareh, N. Gathercole, *Energy Environ. Sci.* **2018**, *11*, 2919.

[26] S. Chun, A. Hong, Y. Choi, C. Ha, W. Park, *Nanoscale* **2016**, *8*, 9185.

[27] J. Li, S. Orrego, J. Pan, P. He, S. H. Kang, *Nanoscale* **2019**, *11*, 2779.

[28] W. R. McCall, K. Kim, C. Heath, G. La Pierre, D. J. Sirbuly, *ACS Appl. Mater. Interfaces* **2014**, *6*, 19504.

[29] Y. Cao, T. Li, Y. Gu, H. Luo, S. Wang, T. Zhang, *Small* **2018**, *14*, 1703902.

[30] M. Ha, S. Lim, J. Park, D.-S. Um, Y. Lee, H. Ko, *Adv. Funct. Mater.* **2015**, *25*, 2841.

[31] M. K. Jonghwa Park, Youngoh Lee, Heon Sang Lee, Hyunhyub Ko, *Sci. Adv.* **2015**, *1*, e1500661.

[32] G. Y. Bae, S. W. Pak, D. Kim, G. Lee, H. Kim do, Y. Chung, K. Cho, *Adv. Mater.* **2016**, *28*, 5300.

[33] C. L. Choong, M. B. Shim, B. S. Lee, S. Jeon, D. S. Ko, T. H. Kang, J. Bae, S. H. Lee, K. E. Byun, J. Im, Y. J. Jeong, C. E. Park, J. J. Park, U. I. Chung, *Adv. Mater.* **2014**, *26*, 3451.

[34] Y. Pang, K. Zhang, Z. Yang, S. Jiang, Z. Ju, Y. Li, X. Wang, D. Wang, M. Jian, Y. Zhang, R. Liang, H. Tian, Y. Yang, T. L. Ren, *ACS Nano* **2018**, *12*, 2346.

[35] J. Lee, H. Kwon, J. Seo, S. Shin, J. H. Koo, C. Pang, S. Son, J. H. Kim, Y. H. Jang, D. E. Kim, T. Lee, *Adv. Mater.* **2015**, *27*, 2433.

[36] G. Z. Li, G. G. Wang, D. M. Ye, X. W. Zhang, Z. Q. Lin, H. L. Zhou, F. Li, B. L. Wang, J. C. Han, *Adv. Electron. Mater.* **2019**, *5*, 1800846.

[37] S. Wang, D. Li,Y. Zhou, L. Jiang, *ACS Nano*, **2020**, *14*, 8634.

[38] S. Garain, S. Jana, T. K. Sinha, D. Mandal, *ACS Appl. Mater. Interfaces* **2016**, *8*, 4532.

[39] X. Zhang, L. Lu, W. Wang, N. Zhao, P. He, J. Liu, B. Yang, *ACS Appl. Mater. Interfaces* **2022**, *14*, 38409.

[40] S. Kim, M. Amjadi, T. I. Lee, Y. Jeong, D. Kwon, M. S. Kim, K. Kim, T. S. Kim, Y. S. Oh, I. Park, *ACS Appl. Mater. Interfaces* **2019**, *11*, 23639.

[41] Y. Hou, L. Wang, R. Sun, Y. Zhang, M. Gu, Y. Zhu, Y. Tong, X. Liu, Z. Wang, J. Xia, Y. Hu, L. Wei, C. Yang, M. Chen, *ACS Nano* **2022**, *16*, *8358*.

[42] Y. Huan, X. Zhang, J. Song, Y. Zhao, T. Wei, G. Zhang, X. Wang, *Nano Energy* **2018**, *50*, 62.

[43] J. Jeon, H. B. Lee, Z. Bao, *Adv. Mater.* **2013**, *25*, 850.

[44] D. Lee, H. Lee, Y. Jeong, Y. Ahn, G. Nam, Y. Lee, *Adv. Mater.* **2016**, *28*, 9364.

[45] S. Cheon, H. Kang, H. Kim, Y. Son, J. Y. Lee, H.-J. Shin, S.-W. Kim, J. H. Cho, *Adv. Funct. Mater.* **2018**, *28*, 1703778.

[46] B. Dudem, D. H. Kim, L. K. Bharat, J. S. Yu, *Appl. Energy* **2018**, *230*, 865.

[47] X. Chen, X. Li, J. Shao, N. An, H. Tian, C. Wang, T. Han, L. Wang, B. Lu, *Small* **2017**, *13*, 1604245.

[48] L. Pan, A. Chortos, G. Yu, Y. Wang, S. Isaacson, R. Allen, Y. Shi, R. Dauskardt, Z. Bao, *Nat. Commun.* **2014**, *5*, 3002.

[49] M. Z. Seyedin, J. M. Razal, P. C. Innis, G. G. Wallace, *Adv. Funct. Mater.* **2014**, *24*, 2957.

[50] Z. Wang, S. Wang, J. Zeng, X. Ren, A. J. Chee, B. Y. Yiu, W. C. Chung, Y. Yang, A. C. Yu, R. C. Roberts, A. C. Tsang, K. W. Chow, P. K. Chan, *Small* **2016**, *12*, 3827.

[51] W. Gao, H. Ota, D. Kiriya, K. Takei, A. Javey, *Acc. Chem. Res.* **2019**, *52*, 523.

[52] D. Qi, K. Zhang, G. Tian, B. Jiang, Y. Huang, *Adv. Mater.* **2020**, e2003155.

[53] X. Wang, Z. Liu, T. Zhang, *Small* **2017**, *13*, 1602790.

[54] A. P. Morteza Amjadi, Sangjun Lee, Seunghwa Ryu, Inkyu Park, *ACS Nano* **2014**, *8*, 5154.

[55] Y. Li, D. Han, C. Jiang, E. Xie, W. Han, *Adv. Mater. Technol.* **2019**, *4*, 1800504.

[56] K. Y. Chun, Y. Oh, J. Rho, J. H. Ahn, Y. J. Kim, H. R. Choi, S. Baik, *Nat. Nanotechnol.* **2010**, *5*, 853.

[57] D. J. Lipomi, M. Vosgueritchian, B. C. Tee, S. L. Hellstrom, J. A. Lee, C. H. Fox, Z. Bao, *Nat. Nanotechnol.* **2011**, *6*, 788.

[58] S. Littlejohn, A. Nogaret, G. M. Prentice, G. D. Pantos, *Adv. Funct. Mater.* **2013**, *23*, 5398.

[59] Y. A. Samad, Y. Li, A. Schiffer, S. M. Alhassan, K. Liao, *Small* **2015**, *11*, 2380.

[60] X. Wu, Y. Han, X. Zhang, Z. Zhou, C. Lu, *Adv. Funct. Mater.* **2016**, *26*, 6246.

[61] Y. Chen, L. Wang, Z. Wu, J. Luo, B. Li, X. Huang, H. Xue, J. Gao, *Compos. B Eng.* **2019**, *176*, 107358.

[62] M. Qu, Y. Qin, Y. Sun, H. Xu, D. W. Schubert, K. Zheng, W. Xu, F. Nilsson, *ACS Appl. Mater. Interfaces* **2020**, *12*, 42140.

[63] Z. Wang, X. Guan, H. Huang, H. Wang, W. Lin, Z. Peng, *Adv. Funct. Mater.* **2019**, *29*,

[64] T. Yokota, Y. Inoue, Y. Terakawa, J. Reeder, M. Kaltenbrunner, T. Ware, K. Yang, K. Mabuchi, T. Murakawa, M. Sekino, W. Voit, T. Sekitani, T. Someya, *Proc. Natl. Acad. Sci. U. S. A.* **2015**, *112*, 14533.

[65] Q. J. Sun, J. Zhuang, S. Venkatesh, Y. Zhou, S. T. Han, W. Wu, K. W. Kong, W. J. Li, X. Chen, R. K. Y. Li, V. A. L. Roy, *ACS Appl. Mater. Interfaces* **2018**, *10*, 4086.

[66] Q. J. Sun, X. H. Zhao, Y. Zhou, C. C. Yeung, W. Wu, S. Venkatesh, Z. X. Xu, J. J. Wylie, W. J. Li, V. A. L. Roy, *Adv. Funct. Mater.* **2019**, *29*, 1808829.

[67] A. K. G. A. K. S. Novoselov, *Nat. Mater.* **2007**, *6*, 183.

[68] A. K. G. K. S. Novoselov, S. V. Morozov, D. Jiang, Y. Zhang, S. V. Dubonos, I. V. Grigorieva, A. A. Firsov, *Science* **2004**, *306*, 666.

[69] X. Cao, J. Zhang, S. Chen, R. J. Varley, K. Pan, *Adv. Funct. Mater.* **2020**, *30*, 2003618.

[70] H. B. Yao, J. Ge, C. F. Wang, X. Wang, W. Hu, Z. J. Zheng, Y. Ni, S. H. Yu, *Adv. Mater.* **2013**, *25*, 6692.

[71] S. Lee, A. Reuveny, J. Reeder, S. Lee, H. Jin, Q. Liu, T. Yokota, T. Sekitani, T. Isoyama, Y. Abe, Z. Suo, T. Someya, *Nat. Nanotechnol.* **2016**, *11*, 472.

[72] J. Chen, Y. Zhu, W. Jiang, *Compos. Sci. Technol.* **2020**, *186*, 107938.

[73] L. Miao, J. Wan, Y. Song, H. Guo, H. Chen, X. Cheng, H. Zhang, *ACS Appl. Mater. Interfaces* **2019**, *11*, 39219.

[74] Z. Pei, Y. Liu, Q. Zhang, D. Zhao, J. Wang, Z. Yuan, W. Zhang, S. Sang, *Adv. Electron. Mater.* **2019**, *5*, 1900227.

[75] X. Han, H. Zhang, W. Xiao, X. Han, A. He, H. Nie,, *J. Mater. Chem. A* **2021**, *9*, 4317.

[76] J. Wu, H. Li, X. Lai, Z. Chen, X. Zeng, *Chem. Eng. J.* **2020**, *386*, 123998.

[77] J. Park, Y. Lee, J. Hong, M. Ha, Y. Jung, H. Lim, S. Y. Kim, H. Ko, *ACS Nano* **2014**, *8*, 4689.

[78] H. Le Ferrand, A. R. Studart, A. F. Arrieta, *ACS Nano* **2019**, *13*, 4752.

[79] C. Pang, G. Y. Lee, T. I. Kim, S. M. Kim, H. N. Kim, S. H. Ahn, K. Y. Suh, *Nat. Mater.* **2012**, *11*, 795.

[80] M. Park, J. Park, U. Jeong, *Nano Today* **2014**, *9*, 244.

[81] K. Takei, Z. Yu, M. Zheng, H. Ota, T. Takahashi, A. Javey, *Proc. Natl. Acad. Sci. U. S. A.* **2014**, *111*, 1703.

[82] Y. J. Tsai, C. M. Wang, T. S. Chang, S. Sutradhar, C. W. Chang, C. Y. Chen, C. H. Hsieh, W. S. Liao, *ACS Appl. Mater. Interfaces* **2019**, *11*, 10380.

[83] Z. Wang, L. Zhang, J. Liu, C. Li, *Nanoscale* **2019**, *11*, 14242.

[84] L. Wang, M. Xia, D. Wang, J. Yan, X. Huang, J. Luo, H. Xue, J. Gao, *ACS Sustainable Chem. Eng.* **2021**, *9*, 7245.

[85] C. Xu, Z. Zheng, M. Lin, Q. Shen, X. Wang, B. Lin, L. Fu, *ACS Appl. Mater. Interfaces* **2020**, *12*, 35482.

[86] S. Jeong, S. Jung, H. Kang, D. Lee, S.-B. Choi, S. Kim, B. Park, K. Yu, J. Lee, K. Lee, *Adv. Funct. Mater.* **2017**, *27*, 1606842.

[87] Y. W. Lim, J. Jin, B. S. Bae, *Adv. Mater.* **2020**, *32*, e1907143.

[88] Z. Liu, G. Chen, *Adv. Mater. Technol.* **2020**, *5*, 2000049.

[89] Y. Liu, K. He, G. Chen, W. R. Leow, X. Chen, *Chem. Rev.* **2017**, *117*, 12893.

[90] I. Kim, K. Woo, Z. Zhong, P. Ko, Y. Jang, M. Jung, J. Jo, S. Kwon, S. H. Lee, S. Lee, H. Youn, J. Moon, *Nanoscale* **2018**, *10*, 7890.

[91] W. Guo, P. Zheng, X. Huang, H. Zhuo, Y. Wu, Z. Yin, Z. Li, H. Wu, *ACS Appl. Mater. Interfaces* **2019**, *11*, 8567.

[92] G. W. Huang, N. Li, Y. Liu, C. B. Qu, Q. P. Feng, H. M. Xiao, *ACS Appl. Mater. Interfaces* **2019**, *11*, 15028.

[93] B. Zhu, Y. Ling, L. W. Yap, M. Yang, F. Lin, S. Gong, Y. Wang, T. An, Y. Zhao, W. Cheng, *ACS Appl. Mater. Interfaces* **2019**, *11*, 29014.

[94] S. Wang, Y. Cheng, R. Wang, J. Sun, L. Gao, *ACS Appl. Mater. Interfaces* **2014**, *6*, 6481.

[95] S. M. Jung, D. J. Preston, H. Y. Jung, Z. Deng, E. N. Wang, J. Kong, *Adv. Mater.* **2016**, *28*, 1413.

[96] K. H. Kim, N. S. Jang, S. H. Ha, J. H. Cho, J. M. Kim, *Small* **2018**, *14*, e1704232.

[97] J. Li, S. Chen, W. Liu, R. Fu, S. Tu, Y. Zhao, L. Dong, B. Yan, Y. Gu, *J. Phys. Chem. C* **2019**, *123*, 11378.

[98] B. Liu, S. Wang, Z. Yuan, Z. Duan, Q. Zhao, Y. Zhang, Y. Su, Y. Jiang, G. Xie, H. Tai, *Nano Energy* **2020**, *78*, 105256.

[99] X. Guan, B. Xu, J. Gong, *Nano Energy* **2020**, *70*, 104516.

[100] S. Paria, S. Ojha, S. K. Karan, S. K. Si, R. Bera, A. K. Das, A. Maitra, L. Halder, A. De, B. B. Khatua, *ACS Appl. Electron. Mater.* **2020**, *2*, 2565.

[101] A. Rovisco, A. Dos Santos, T. Cramer, J. Martins, R. Branquinho, H. Aguas, B. Fraboni, E. Fortunato, R. Martins, R. Igreja, P. Barquinha, *ACS Appl. Mater. Interfaces* **2020**, *12*, 18421.

[102] J. Chun, N.-R. Kang, J.-Y. Kim, M.-S. Noh, C.-Y. Kang, D. Choi, S.-W. Kim, Z. Lin Wang, J. Min Baik, *Nano Energy* **2015**, *11*, 1.

[103] K. Shi, X. Huang, B. Sun, Z. Wu, J. He, P. Jiang, *Nano Energy* **2019**, *57*, 450.

[104] Y. Ding, J. Yang, C. R. Tolle, Z. Zhu, *ACS Appl. Mater. Interfaces* **2018**, *10*, 16077.

[105] H. Park, Y. R. Jeong, J. Yun, S. Y. Hong, S. Jin, S. Lee, G. Zi, J. S. Ha, *ACS Nano* **2015**, *9*, 9974.

[106] C. Merlini, G. M. O. Barra, T. Medeiros Araujo, A. Pegoretti, *RSC Adv.* **2014**, *4*, 15749.

[107] Y.-T. Tseng, Y.-C. Lin, C.-C. Shih, H.-C. Hsieh, W.-Y. Lee, Y.-C. Chiu, W.-C. Chen, *J. Mater. Chem. C* **2020**, *8*, 6013.

[108] Z. Wen, Y. Yang, N. Sun, G. Li, Y. Liu, C. Chen, J. Shi, L. Xie, H. Jiang, D. Bao, Q. Zhuo, X. Sun, *Adv. Funct. Mater.* **2018**, *28*, 1803684.

[109] C. Yang, L. Li, J. Zhao, J. Wang, J. Xie, Y. Cao, M. Xue, C. Lu, *ACS Appl. Mater. Interfaces* **2018**, *10*, 25811.

[110] Y. Yu, S. Peng, P. Blanloeuil, S. Wu, C. H. Wang, *ACS Appl. Mater. Interfaces* **2020**, *12*, 36578.

[111] M. Lou, I. Abdalla, M. Zhu, J. Yu, Z. Li, B. Ding, *ACS Appl. Mater. Interfaces* **2020**, *12*, 1597.

[112] Q. Wu, Y. Qiao, R. Guo, S. Naveed, T. Hirtz, X. Li, Y. Fu, Y. Wei, G. Deng, Y. Yang, X. Wu, T. L. Ren, *ACS Nano* **2020**, *14*, 10104.

[113] Y. Xiong, Y. Shen, L. Tian, Y. Hu, P. Zhu, R. Sun, C.-P. Wong, *Nano Energy* **2020**, *70*, 104436.

[114] J. Chen, J. Liu, T. Thundat, H. Zeng, *ACS Appl. Mater. Interfaces* **2019**, *11*, 18720.

[115] T. P. Huynh, P. Sonar, H. Haick, *Adv. Mater.* **2017**, *29*, 1604973.

[116] X. Xun, Z. Zhang, X. Zhao, B. Zhao, F. Gao, Z. Kang, Q. Liao, Y. Zhang, *ACS Nano* **2020**, *14*, 9066.

[117] K. Parida, J. Xiong, X. Zhou, P. S. Lee, *Nano Energy* **2019**, *59*, 237.

[118] T. Wang, Y. Zhang, Q. Liu, W. Cheng, X. Wang, L. Pan, B. Xu, H. Xu, *Adv. Funct. Mater.* **2018**, *28*, 1705551.

[119] L. Pan, G. Yu, D. Zhai, H. R. Lee, W. Zhao, N. Liu, H. Wang, B. C. Tee, Y. Shi, Y. Cui, Z. Bao, *Proc. Natl. Acad. Sci. U. S. A.* **2012**, *109*, 9287.

[120] C. S. Luo, P. Wan, H. Yang, S. A. A. Shah, X. Chen, *Adv. Funct. Mater.* **2017**, *27*, 1606339.

[121] D. L. Taylor, M. In Het Panhuis, *Adv. Mater.* **2016**, *28*, 9060.

[122] L. Lan, F. Zhao, Y. Yao, J. Ping, Y. Ying, *ACS Appl. Mater. Interfaces* **2020**, *12*, 10689.

[123] L. Wang, D. Wang, Z. Wu, J. Luo, X. Huang, Q. Gao, X. Lai, L. C. Tang, H. Xue, J. Gao, *ACS Appl. Mater. Interfaces* **2020**, *12*, 13316.

[124] Q.-J. Sun, J. Peng, W.-H. Chen, X.-J. She, J. Liu, X. Gao, W.-L. Ma, S.-D. Wang, *Org. Electron.* **2016**, *34*, 118.

[125] J. Koo, J. Yang, B. Cho, H. Jo, K. H. Lee, M. S. Kang, *ACS Appl. Mater. Interfaces* **2018**, *10*, 9563.

[126] W. L. Leong, N. Mathews, B. Tan, S. Vaidyanathan, F. Dötz, S. Mhaisalkar, *J. Mater. Chem.* **2011**, *21*, 5203.

[127] S. Zhang, H. Liu, S. Yang, X. Shi, D. Zhang, C. Shan, L. Mi, C. Liu, C. Shen, Z. Guo, *ACS Appl. Mater. Interfaces* **2019**, *11*, 10922.

[128] I. M. Asuo, P. Fourmont, I. Ka, D. Gedamu, S. Bouzidi, A. Pignolet, R. Nechache, S. G. Cloutier, *Small* **2019**, *15*, e1804150.

[129] S. R. A. Ruth, L. Beker, H. Tran, V. R. Feig, N. Matsuhisa, Z. Bao, *Adv. Funct. Mater.* **2019**, *30*, 1903100.

[130] Q.-J. Sun, J. Zhuang, Y. Yan, L. Zhou, Y. Zhou, S.-T. Han, W. Wu, H.-Y. Peng, R. K. Y. Li, A. L. R. Vellaisamy, *Phys. Status Solidi A* **2016**, *213*, 2509.

[131] Q.-J. Sun, J. Zhuang, Y. Yan, Y. Zhou, S.-T. Han, L. Zhou, V. A. L. Roy, *Phys. Status Solidi A* **2016**, *213*, 79.

[132] J. Tao, Z. Xiao, J. Wang, C. Li, X. Sun, F. Li, X. Zou, G. Liao, Z. Zou, *J. Alloys. Compd.* **2020**, *845*, 155311.

[133] Q. Xie, L. Wang, Y. Zhu, Q. Sun, L. Wang, *Org. Electron.* **2019**, *74*, 69.

[134] Q. Zhou, B. Ji, Y. Wei, B. Hu, Y. Gao, Q. Xu, J. Zhou, B. Zhou, *J. Mater. Chem. A* **2019**, *7*, 27334.

[135] R. Bao, C. Wang, L. Dong, R. Yu, K. Zhao, Z. L. Wang, C. Pan, *Adv. Funct. Mater.* **2015**, *25*, 2884.

[136] Y. H. Chou, Y. C. Chiu, W. C. Chen, *Chem. Commun.* **2014**, *50*, 3217.

[137] Y. Zhou, S. T. Han, Z. X. Xu, V. A. Roy, *Nanotechnology* **2012**, *23*, 344014.

[138] L. Li, Y. Bai, L. Li, S. Wang, T. Zhang, *Adv. Mater.* **2017**, *29*, 1702517.

[139] H. H. Chou, A. Nguyen, A. Chortos, J. W. To, C. Lu, J. Mei, T. Kurosawa, W. G. Bae, J. B. Tok, Z. Bao, *Nat. Commun.* **2015**, *6*, 8011.

[140] J. Ma, P. Wang, H. Chen, S. Bao, W. Chen, H. Lu, *ACS Appl. Mater. Interfaces* **2019**, *11*, 8527.

[141] W. Wu, *Sci. Technol. Adv. Mater.* **2019**, *20*, 187.

[142] S. Yao, Y. Zhu, *Nanoscale* **2014**, *6*, 2345.

[143] H. Shi, M. Al‐Rubaiai, C. M. Holbrook, J. Miao, T. Pinto, C. Wang, X. Tan, *Adv. Funct. Mater.* **2019**, *29*, 1809116.

[144] P. Wei, X. Yang, Z. Cao, X. L. Guo, H. Jiang, Y. Chen, M. Morikado, X. Qiu, D. Yu, *Adv. Mater. Technol.* **2019**, *4*, 1900315.

[145] S. Khan, S. Tinku, L. Lorenzelli, R. S. Dahiya, *IEEE Sens. J.* **2015**, *15*, 3146.

[146] Y. Gao, G. Yu, T. Shu, Y. Chen, W. Yang, Y. Liu, J. Long, W. Xiong, F. Xuan, *Adv. Mater. Technol.* **2019**, *4*, 1900504.

[147] D. Maurya, S. Khaleghian, R. Sriramdas, P. Kumar, R. A. Kishore, M. G. Kang, V. Kumar, H. C. Song, S. Y. Lee, Y. Yan, J. M. Park, S. Taheri, S. Priya, *Nat. Commun.* **2020**, *11*, 5392.

[148] S. Mousavi, D. Howard, F. Zhang, J. Leng, C. H. Wang, *ACS Appl. Mater. Interfaces* **2020**, *12*, 15631.

[149] Z. Tang, S. Jia, C. Zhou, B. Li, *ACS Appl. Mater. Interfaces* **2020**, *12*, 28669.

[150] X.-Y. Yin, Y. Zhang, X. Cai, Q. Guo, J. Yang, Z. L. Wang, *Materials Horizons* **2019**, *6*, 767.

[151] Y. Ko, D. Kim, U. J. Kim, J. You, *Carbohydr. Polym.* **2017**, *173*, 383.

[152] L. Lan, T. Yin, C. Jiang, X. Li, Y. Yao, Z. Wang, S. Qu, Z. Ye, J. Ping, Y. Ying, *Nano Energy* **2019**, *62*, 319.

[153] C. Yan, J. Wang, W. Kang, M. Cui, X. Wang, C. Y. Foo, K. J. Chee, P. S. Lee, *Adv. Mater.* **2014**, *26*, 2022.

[154] B. Azimi, M. Milazzo, A. Lazzeri, S. Berrettini, M. J. Uddin, Z. Qin, M. J. Buehler, S. Danti, *Adv. Healthc. Mater.* **2020**, *9*, 1901287.

[155] S. Kalani, R. Kohandani, R. Bagherzadeh, *RSC Adv.* **2020**, *10*, 35090.

[156] L. Lu, B. Yang, Y. Zhai, J. Liu, *Nano Energy* **2020**, *76*, 104966.

[157] K. Shi, B. Sun, X. Huang, P. Jiang, *Nano Energy* **2018**, *52*, 153.

[158] C. Jiang, C. Wu, X. Li, Y. Yao, L. Lan, F. Zhao, Z. Ye, Y. Ying, J. Ping, *Nano Energy* **2019**, *59*, 268.

[159] I. P. Chen, M. C. Yang, C. H. Yang, D. X. Zhong, M. C. Hsu, Y. Chen, *ACS Appl. Mater. Interfaces* **2017**, *9*, 5550.

[160] M. Ding, L. Jing, H. Yang, C. E. Machnicki, X. Fu, K. Li, I. Y. Wong, P. Y. Chen, *Materials Today Advances* **2020**, *8*, 100088.

[161] U. Kalsoom, S. Waheed, B. Paull, *ACS Appl. Mater. Interfaces* **2020**, *12*, 4962.

[162] M. Kim, D. Park, M. M. Alam, S. Lee, P. Park, J. Nah, *ACS Nano* **2019**, *13*, 4640.

[163] Z. Liu, Z. Yin, S.-C. Chen, S. Dai, J. Huang, Q. Zheng, *Org. Electron.* **2018**, *53*, 205.

[164] T. Wu, E. Gray, B. Chen, *J. Mater. Chem. C* **2018**, *6*, 6200.

[165] S. Ji, J. Jang, J. C. Hwang, Y. Lee, J. H. Lee, J. U. Park, *Adv. Mater. Technol.* **2019**, *5*, 1900928.

[166] X. Li, Y. J. Fan, H. Y. Li, J. W. Cao, Y. C. Xiao, Y. Wang, F. Liang, H. L. Wang, Y. Jiang, Z. L. Wang, G. Zhu, *ACS Nano* **2020**, *14*, 9605.

[167] C. Zhang, S. Liu, X. Huang, W. Guo, Y. Li, H. Wu, *Nano Energy* **2019**, *62*, 164.

[168] L. Bi, Z. Yang, L. Chen, Z. Wu, C. Ye, *J. Mater. Chem. A* **2020**, *8*, 20030.

[169] E. S. Hosseini, L. Manjakkal, D. Shakthivel, R. Dahiya, *ACS Appl. Mater. Interfaces* **2020**, *12*, 9008.

[170] S. Sharma, A. Chhetry, M. Sharifuzzaman, H. Yoon, J. Y. Park, *ACS Appl. Mater. Interfaces* **2020**, *12*, 22212.

[171] W. Chen, X. Yan, *J. Mater. Sci. Technol.* **2020**, *43*, 175.

[172] Y. Zang, F. Zhang, C.-a. Di, D. Zhu, *Mater. Horiz.* **2015**, *2*, 140.

[173] K. Liu, Z. Zhou, X. Yan, X. Meng, H. Tang, K. Qu, Y. Gao, Y. Li, J. Yu, L. Li, *Polymers* **2019**, *11*, 1120.

[174] Q. Liu, Z. Liu, C. Li, K. Xie, P. Zhu, B. Shao, J. Zhang, J. Yang, J. Zhang, Q. Wang, C. F. Guo, *Adv. Sci.* **2020**, *7*, 2000348.

[175] X. Tang, C. Wu, L. Gan, T. Zhang, T. Zhou, J. Huang, H. Wang, C. Xie, D. Zeng, *Small* **2019**, *15*, 1804559.

[176] J. Xu, H. Wang, T. Ma, Y. Wu, R. Xue, H. Cui, X. Wu, Y. Wang, X. Huang, W. Yao, *Carbon* **2020**, *166*, 316.

[177] G. Shen, B. Chen, T. Liang, Z. Liu, S. Zhao, J. Liu, C. Zhang, W. Yang, Y. Wang, X. He, *Adv. Electron. Mater.* **2020**, *6*, 1901360.

[178] J. Chen, Q. Yu, X. Cui, M. Dong, J. Zhang, C. Wang, J. Fan, Y. Zhu, Z. Guo, *J. Mater. Chem. C* **2019**, *7*, 11710.

[179] T. Yamada, Y. Hayamizu, Y. Yamamoto, Y. Yomogida, A. Izadi-Najafabadi, D. N. Futaba, K. Hata, *Nat. Nanotechnol.* **2011**, *6*, 296.

[180] X. Liao, Z. Zhang, Z. Kang, F. Gao, Q. Liao, Y. Zhang, *Mater. Horiz.* **2017**, *4*, 502.

[181] Y. Tang, Z. Zhao, H. Hu, Y. Liu, X. Wang, S. Zhou, J. Qiu, *ACS Appl. Mater. Interfaces* **2015**, *7*, 27432.

[182] S. Gong, D. T. H. Lai, B. Su, K. J. Si, Z. Ma, L. W. Yap, P. Guo, W. Cheng, *Adv. Electron. Mater.* **2015**, *1*, 1400063.

[183] C. Wang, X. Li, E. Gao, M. Jian, K. Xia, Q. Wang, Z. Xu, T. Ren, Y. Zhang, *Adv. Mater.* **2016**, *28*, 6640.

[184] C. Wang, K. Xia, M. Zhang, M. Jian, Y. Zhang, *ACS Appl. Mater. Interfaces* **2017**, *9*, 39484.

[185] Z. Han, H. Li, J. Xiao, H. Song, B. Li, S. Cai, Y. Chen, Y. Ma, X. Feng, *ACS Appl. Mater. Interfaces* **2019**, *11*, 33370.

[186] D. Wang, L. Wang, Z. Lou, Y. Zheng, K. Wang, L. Zhao, W. Han, K. Jiang, G. Shen, *Nano Energy* **2020**, *78*, 105252.

[187] Y. Qiu, Y. Tian, S. Sun, J. Hu, Y. Wang, Z. Zhang, A. Liu, H. Cheng, W. Gao, W. Zhang, H. Chai, H. Wu, *Nano Energy* **2020**, *78*, 105337.

[188] L. Shi, Z. Li, M. Chen, Y. Qin, Y. Jiang, L. Wu, *Nat. Commun.* **2020**, *11*, 3529.

[189] Z. Lou, S. Chen, L. Wang, K. Jiang, G. Shen, *Nano Energy* **2016**, *23*, 7.

[190] G. Y. Bae, J. T. Han, G. Lee, S. Lee, S. W. Kim, S. Park, J. Kwon, S. Jung, K. Cho, *Adv. Mater.* **2018**, *30*, 1803388.

[191] S. Han, F. Jiao, Z. U. Khan, J. Edberg, S. Fabiano, X. Crispin, *Adv. Funct. Mater.* **2017**, *27*, 1703549.

[192] D. Katerinopoulou, P. Zalar, J. Sweelssen, G. Kiriakidis, C. Rentrop, P. Groen, G. H. Gelinck, J. van den Brand, E. C. P. Smits, *Adv. Electron. Mater.* **2019**, *5*, 1800605.

[193] Q. Li, L. N. Zhang, X. M. Tao, X. Ding, *Adv. Healthc. Mater.* **2017**, *6*, 1601371.

[194] T. Q. Trung, T. M. L. Dang, S. Ramasundaram, P. T. Toi, S. Y. Park, N. E. Lee, *ACS Appl. Mater. Interfaces* **2019**, *11*, 2317.

[195] Y. Yu, Q. Huang, S. Rhodes, J. Fang, L. An, *J. Am. Ceram. Soc.* **2017**, *100*, 592.

[196] K. Kim, M. Jung, B. Kim, J. Kim, K. Shin, O.-S. Kwon, S. Jeon, *Nano Energy* **2017**, *41*, 301.

[197] J. H. Oh, S. Y. Hong, H. Park, S. W. Jin, Y. R. Jeong, S. Y. Oh, J. Yun, H. Lee, J. W. Kim, J. S. Ha, *ACS Appl. Mater. Interfaces* **2018**, *10*, 7263.

[198] W. He, W. Liu, J. Chen, Z. Wang, Y. Liu, X. Pu, H. Yang, Q. Tang, H. Yang, H. Guo, C. Hu, *Nat. Commun.* **2020**, *11*, 4277.

[199] W. Liu, Z. Wang, G. Wang, G. Liu, J. Chen, X. Pu, Y. Xi, X. Wang, H. Guo, C. Hu, Z. L. Wang, *Nat. Commun.* **2019**, *10*, 1426.

[200] Q.-J. Sun, Y. Lei, X.-H. Zhao, J. Han, R. Cao, J. Zhang, W. Wu, H. Heidari, W.-J. Li, Q. Sun, V. A. L. Roy, *Nano Energy* **2021**, *80*, 105521.

[201] M. Choi, G. Murillo, S. Hwang, J. W. Kim, J. H. Jung, C.-Y. Chen, M. Lee, *Nano Energy* **2017**, *33*, 462.

[202] H. Kang, H. Kim, S. Kim, H. J. Shin, S. Cheon, J.-H. Huh, D. Y. Lee, S. Lee, S.-W. Kim, J. H. Cho, *Adv. Funct. Mater.* **2016**, *26*, 7717.

[203] C. Luo, S. Hu, M. Xia, P. Li, J. Hu, G. Li, H. Jiang, W. Zhang, *Energy Technol.* **2018**, *6*, 922.

[204] E. J. Lee, T. Y. Kim, S.-W. Kim, S. Jeong, Y. Choi, S. Y. Lee, *Energy Environ. Sci.* **2018**, *11*, 1425.

[205] J.-S. Im, I.-K. Park, *ACS Appl. Mater. Interfaces* **2018**, *10*, 25660.

[206] R. Wen, J. Guo, A. Yu, J. Zhai, Z. L. Wang, *Adv. Funct. Mater.* **2019**, *29*, 1807655.

[207] Y. J. Fan, X. S. Meng, H. Y. Li, S. Y. Kuang, L. Zhang, Y. Wu, Z. L. Wang, G. Zhu, *Adv. Mater.* **2017**, *29*, 1603115.

[208] H. Oh, S. S. Kwak, B. Kim, E. Han, G. H. Lim, S. W. Kim, B. Lim, *Adv. Funct. Mater.* **2019**, *29*, 1904066.

[209] F. Zhang, Y. Zang, D. Huang, C.-a. Di, D. Zhu, *Nat. Commun.* **2015**, *6*, 8356.

[210] R. Liu, L. Ma, G. Niu, X. Li, E. Li, Y. Bai, G. Yuan, *Adv. Funct. Mater.* **2017**, *27*, 1701635.

[211] M. Yang, X. Hu, Z. Fang, L. Sun, Z. Yuan, S. Wang, W. Hong, X. Chen, D. Yu, *Adv. Funct. Mater.* **2017**, *27*, 1701971.

[212] O. Yassine, O. Shekhah, A. H. Assen, Y. Belmabkhout, K. N. Salama, M. Eddaoudi, *Angew. Chem.* **2016**, *128*, 16111.

[213] X.-H. Zhao, S.-N. Ma, H. Long, H. Yuan, C. Y. Tang, P. K. Cheng, Y. H. Tsang, *ACS Appl. Mater. Interfaces* **2018**, *10*, 3986.

[214] H. Kleemann, K. Krechan, A. Fischer, K. Leo, *Adv. Funct. Mater.* **2020**, *30*, 1907113.

[215] J. W. Park, B. H. Kang, H. J. Kim, *Adv. Funct. Mater.* **2019**, *30*, 1904632.

[216] P. Ma, L. Du, Y. Wang, R. Jiang, Q. Xin, Y. Li, A. Song, *Appl. Phys. Lett.* **2018**, *112*, 023501.

[217] J. Peng, Q. Sun, S. Wang, H.-Q. Wang, W. Ma, *Appl. Phys. Lett.* **2013**, *103*, 061603.

[218] Y. Zhang, Y. Lin, G. He, B. Ge, W. Liu, *ACS Appl. Electron. Mater.* **2020**, *2*, 3728.

[219] M. Zirkl, A. Haase, A. Fian, H. Schön, C. Sommer, G. Jakopic, G. Leising, B. Stadlober, I. Graz, N. Gaar, R. Schwödiauer, S. Bauer-Gogonea, S. Bauer, *Adv. Mater.* **2007**, *19*, 2241.

[220] J. S. Hur, J. O. Kim, H. A. Kim, J. K. Jeong, *ACS Appl. Mater. Interfaces* **2019**, *11*, 21675.

[221] J. Oh, S. Rondeau-Gagné, Y. Chiu, A. Chortos, F. Lissel, G. N. Wang, B. C. Schroeder, T. Kurosawa, J. Lopez, T. Katsumata, J. Xu, C. Zhu, X. Gu, W. Bae, Y. Kim, L. Jin, J. W. Chung, J. B. H. Tok, Z. Bao, *Nature* **2016**, *539*, 411.

[222] J. Xu, S. Wang, G. N. Wang, C. Zhu, S. Luo, L. Jin, X. Gu, S. Chen, V. R. Feig, J. W. F. To, S. Rondeau-Gagné, J. Park, B. C. Schroeder, C. Lu, J. Y. Oh, Y. Wang, Y. H. Kim, H. Yan, R. Sinclair, D. Zhou, G. Xue, B. Murmann, C. Linder, W. Cai, J. B. H. Tok, J. W. Chung, Z. Bao, *Science* **2017**, *355*, 59.

[223] K. Sim, Z. Rao, H. -J. Kim, A. Thukral, H. Shim, C. Yu, *Sci. Adv.* **2019**, *5*, eaav5749.

[224] J. Y. Oh, D. Son, T. Katsumata, Y. Lee, Y. Kim, J. Lopez, H. -C. Wu, J. Kang, J. Park, X. Gu, J. Mun, N. G. Wang, Y. Yin, W. Cai, Y. Yun, J. B.-H. Tok, Z. Bao, *Sci. Adv.* **2019**, *5*, eaav3097.

[225] N. Luo, Y. Huang, J. Liu, S. -C. Chen, C. P. Wong, N. Zhao, *Adv. Mater.* **2017**, *29*, 1702675.

[226] C. Gerlach, D. Krumm, M. Illing, J. Lange, O. Kanoun, S. Odenwald, A. Hubler, *IEEE Sens. J.* **2015**, *15*, 3647.

[227] Y. Guo, M. Zhong, Z. Fang, P. Wan, G. Yu, *Nano Lett.* **2019**, *19*, 1143.

[228] Y. Gao, H. Ota, E. W. Schaler, K. Chen, A. Zhao, W. Gao, H. M. Fahad, Y. Leng, A. Zheng, F. Xiong, C. Zhang, L.-C. Tai, P. Zhao, R. S. Fearing, A. Javey, *Adv. Mater.* **2017**, *29*, 1701985.

[229] H. Wu, H. Guo, Z. Su, M. Shi, X. Chen, X. Cheng, M. Han, H. Zhang, *J. Mater. Chem. A* **2018**, *6*, 20277.

[230] N. Matsuhisa, D. Inoue, P. Zalar, H. Jin, Y. Matsuba, A. Itoh, T. Yokota, D. Hashizume, T. Someya, *Nat. Mater.* **2017**, *16*, 834.

[231] D. Kang, P. V. Pikhitsa, Y. W. Choi, C. Lee, S. S. Shin, L. Piao, B. Park, K.-Y. Suh, T.-i. Kim, M. Choi, *Nature* **2014**, *516*, 222.

[232] Y. Kim, A. Chortos, W. Xu, Y. Liu, J. Y. Oh, D. Son, J. Kang, A. M. Foudeh, C. Zhu, Y. Lee, S. Niu, J. Liu, R. Pfattner, Z. Bao, T. –W. Lee, *Science* **2018**, *360*, 998.

[233] T. Yang, W. Deng, X. Chu, X. Wang, Y. Hu, X. Fan, J. Song, Y. Gao, B. Zhang, G. Tian, D. Xiong, S. Zhong, L. Tang, Y. Hu, W. Yang, *ACS Nano* **2021**, *15*, 11555.

[234] Q. Liu, J. Chen, Y. Li, G. Shi, *ACS Nano* **2016**, *10*, 7901.

Figure 1. An introduction to the functional polymer composites based E-skin and its potential applications in health monitoring and artificial intelligence. a) Reproduced with permission.[7] Copyright 2021, American Chemical Society. b, g) Reproduced with permission.[8] Copyright 2022, Elsevier. c) Reproduced with permission.[232] Copyright 2018, American Association for the Advancement of Science. d) Reproduced with permission.[17] Copyright 2022, Wiley-VCH. e) Reproduced with permission.[14] Copyright 2022, American Association for the Advancement of Science. f) Reproduced with permission.[31] Copyright 2015, American Association for the Advancement of Science. h) Reproduced with permission.[233] Copyright 2021, American Chemical Society. i) Reproduced with permission.[234] Copyright 2016, American Chemical Society.

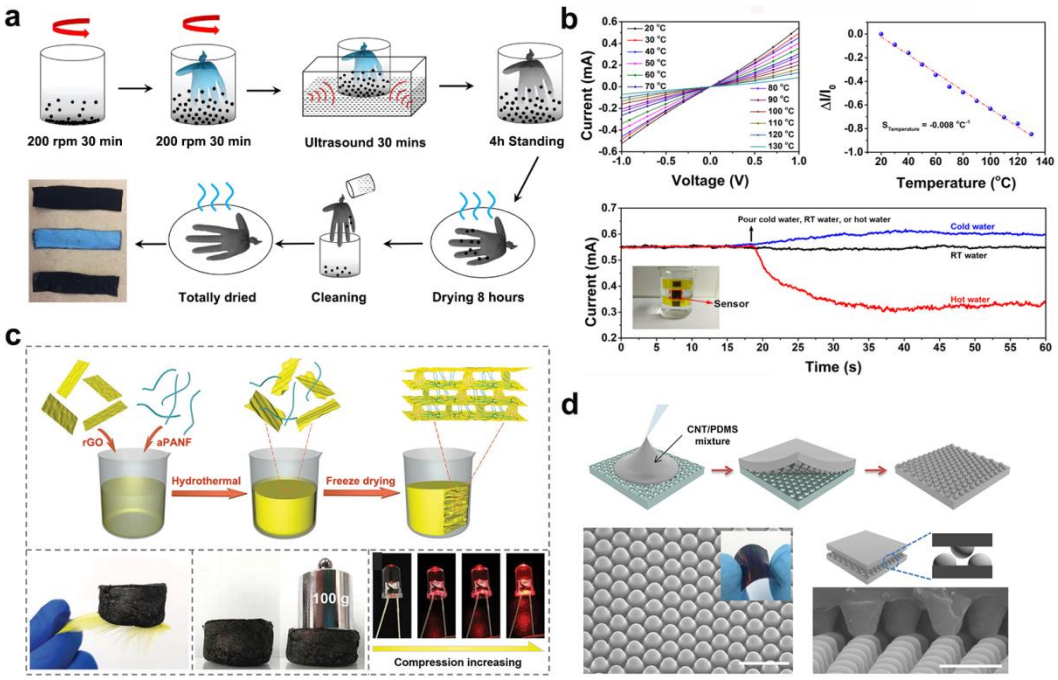

Figure 2. Functional polymer composites with carbon nano-/micro-materials. a) Schematic fabrication process of CB based composite samples. Reproduced with permission.[62] Copyright 2020, American Chemical Society. b) A graphite based composite for temperature sensor. Reproduced with permission.[66] Copyright 2019, Wiley-VCH. c) The fabrication process of aPANF/GA, showing lightweight, excellent mechanical property and good conductivity. Reproduced with permission.[69] Copyright 2020, Wiley-VCH. d) Schematic illustration showing the fabrication of CNTs/PDMS composite with interlocked microdome arrays. SEM images of surface and cross section of the polymer composite. Reproduced with permission.[77] Copyright 2014, American Chemical Society.

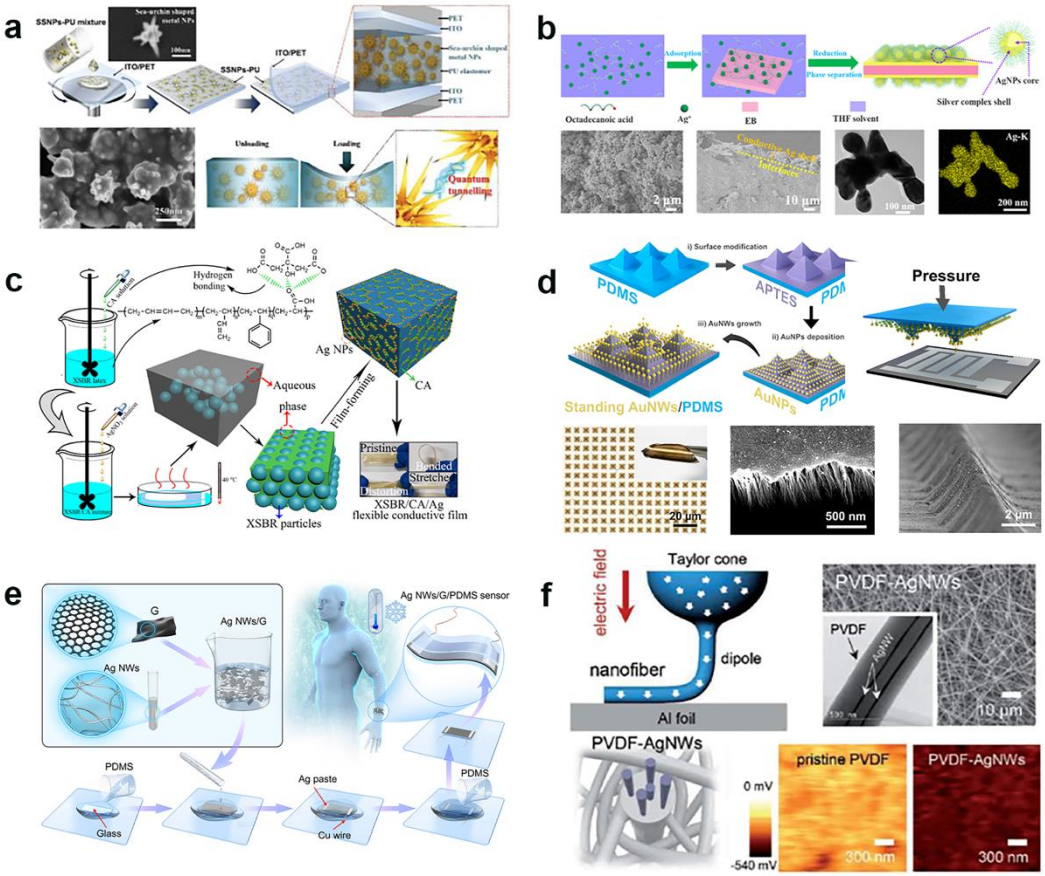

Figure 3. Metal filler based functional polymer composites. a) Schematic illustrating the fabrication process of a transparent polymer composite based on sea-urchin shaped NPs. Reproduced with permission.[44] Copyright 2016, Wiley-VCH. b) Schematic diagram showing in situ preparation of the AgNPs based composite. Reproduced with permission.[84] Copyright 2021, American Chemical Society. c) Multifunctional conductive rubber film based on AgNPs. d) Fabrication of AuNWs based polymer composite. Reproduced with permission.[85] Copyright 2020, American Chemical Society. e) Fabrication of AgNW/PDMS composite film for strain sensors. Reproduced with permission.[96] Copyright 2018, Wiley-VCH. f) AgNWs/PVDF nanofiber based polymer composite for TENGs. Reproduced with permission.[45] Copyright 2018, Wiley-VCH.

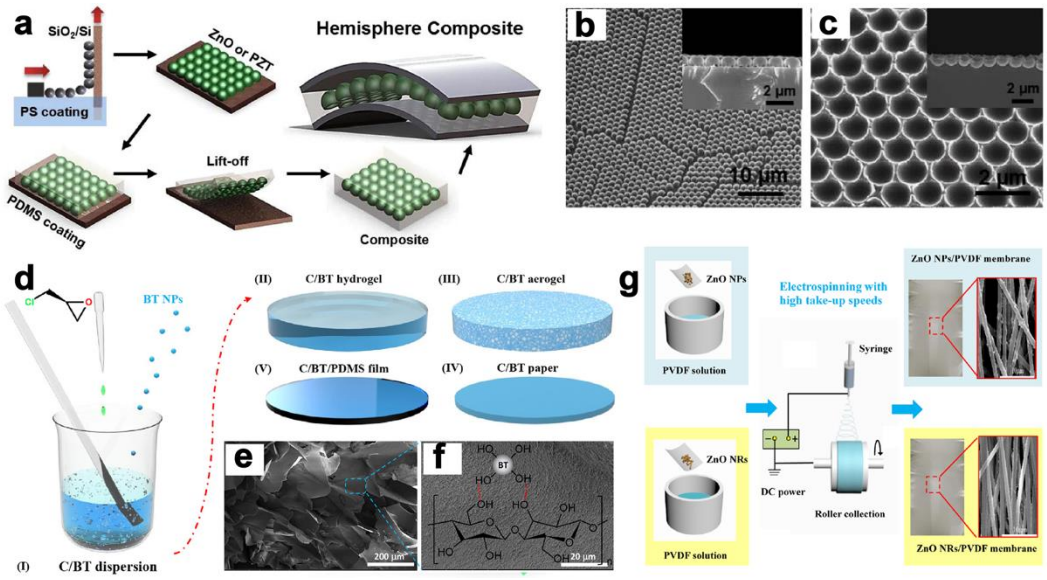

Figure 4. Functional polymer composites based on metal oxide fillers. a) Schematic diagrams of the fabrication process for the piezoelectric hemispheres embedded stretchable composites. SEM images of b) close-packed 2D ZnO hollow hemisphere arrays and c) detached hemisphere array from the substrate. a-c) Reproduced with permission.[102] Copyright 2015, Elsevier. d) Schematic fabrication process of a C/BT aerogel paper. SEM images of e) cross section of the C/BT aerogel and f) magnified C/BT pore wall. d, e, f) Reproduced with permission.[103] Copyright 2019, Elsevier. g) Schematic of the fabrication process of ZnO/PVDF polymer composite via electrospinning. Reproduced with permission.[97] Copyright 2019, American Chemical Society.

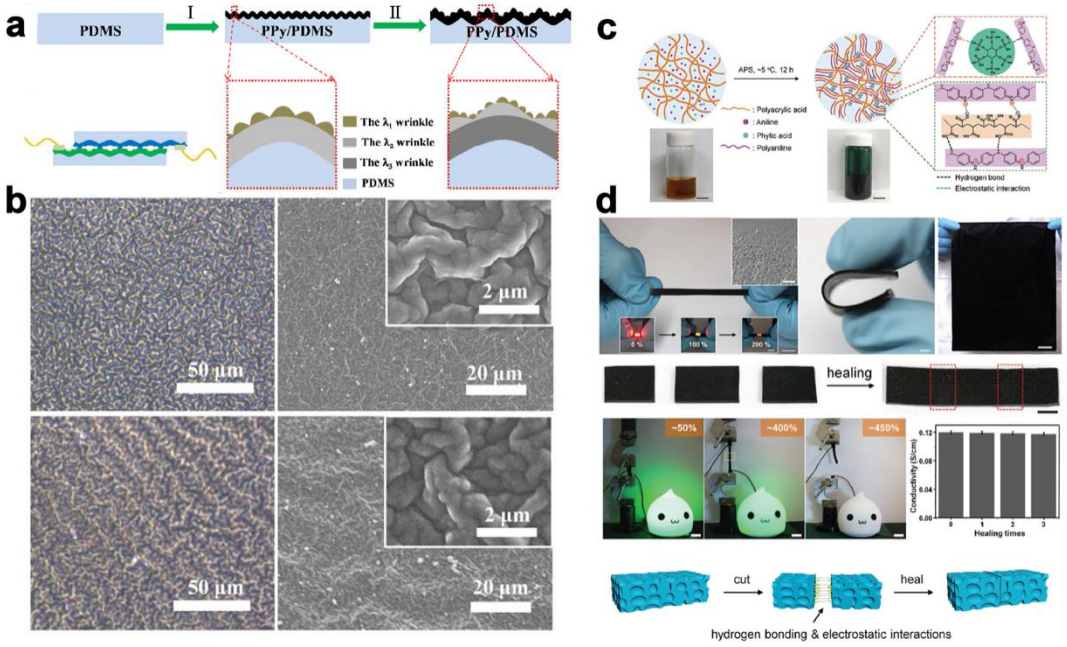

Figure 5. Polymer filler based functional composites. a) Schematic fabrication procedures of the microstructured PPy/PDMS functional composite. b) Optical and SEM images showing nested wrinkling microstructures of PPy/PDMS composite films. Inset showing the magnified SEM images of the composite film. a,b) Reproduced with permission.[109] Copyright 2018, American Chemical Society. c) Schematic showing the synthetic process for the self-healable polymer composite. d) Optical image showing the stretchability, flexibility, and self-healing properties of the polymer composite. The bottom image illustrating the self-healing process due to hydrogen bonding and electrostatic interactions. c,d) Reproduced with permission.[118] Copyright 2018, Wiley-VCH.

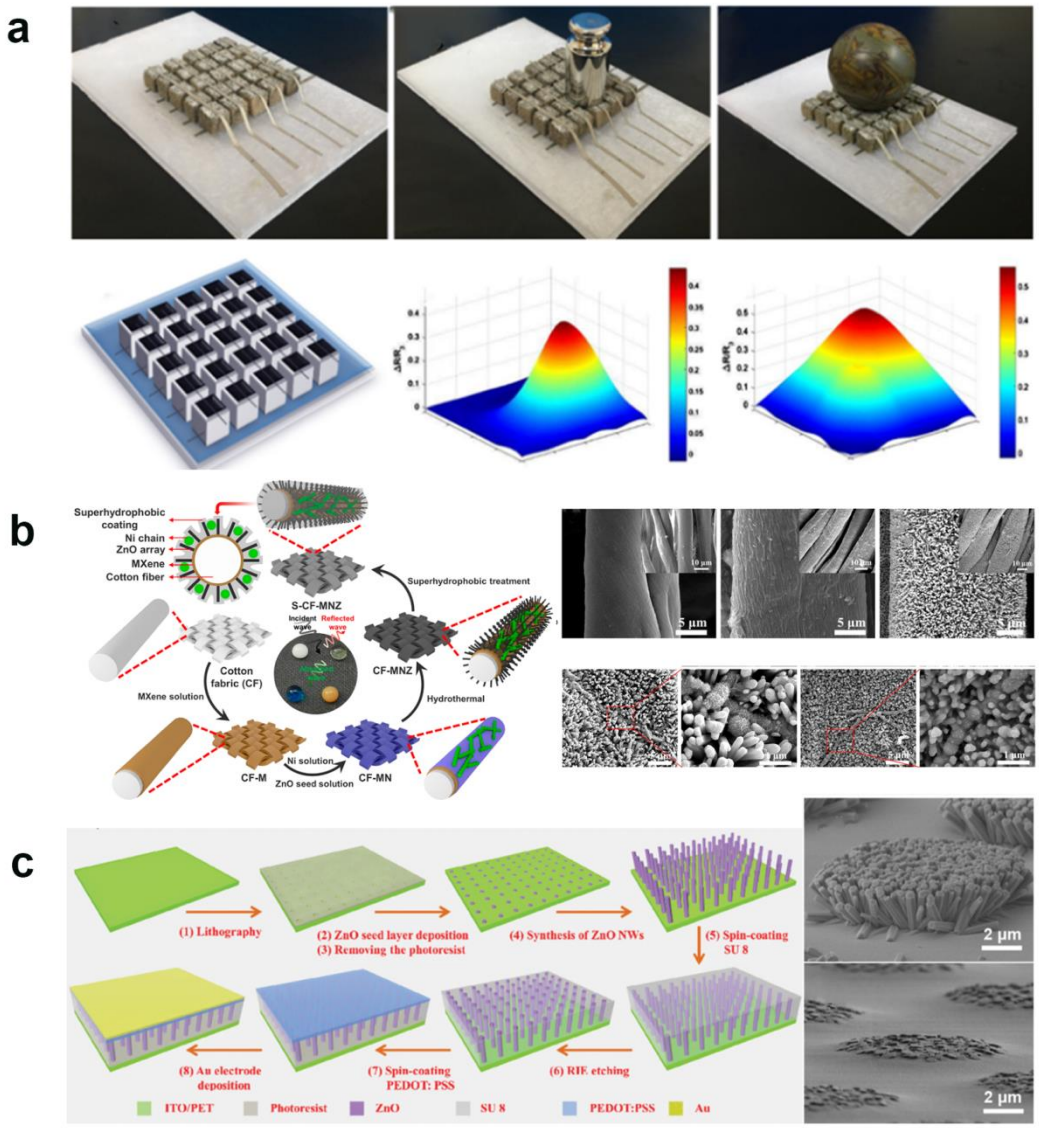

Figure 6. Fabrication technologies for functional polymer composites. a) Pressure sensor arrays with the composite foams fabricated by dip-coating. Reproduced with permission.[127] Copyright 2019, American Chemical Society. b) Preparation of $Ti_3C_2T_x$ MXene/Ni chain/ZnO array hybrid nanostructure. Reproduced with permission.[37] Copyright 2020, American Chemical Society. c) Schematic fabrication procedure of a ZnO NWs/PEDOT:PSS composite array (left) and the SEM image of the ZnO NWs (right). Reproduced with permission.[135] Copyright 2015, Wiley-VCH.

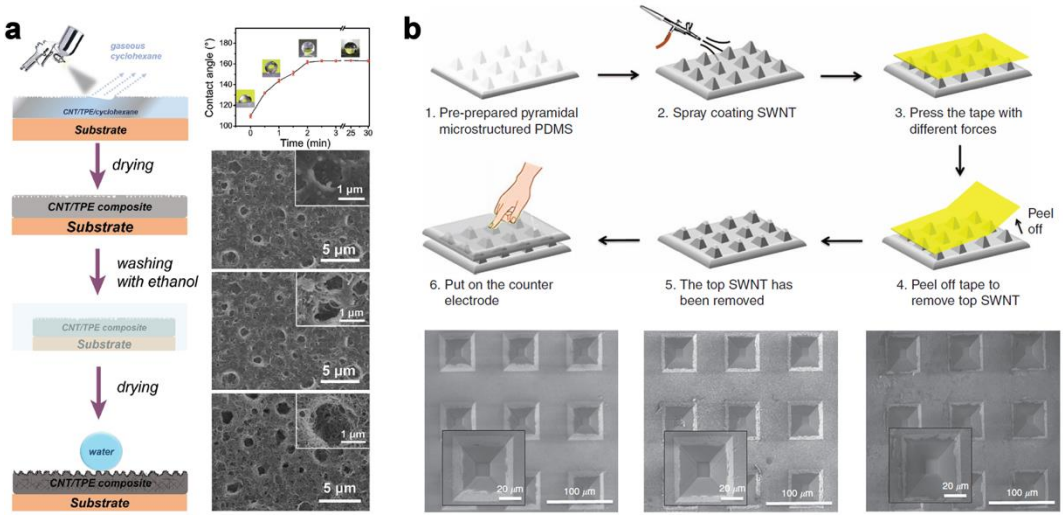

Figure 7. Functional composite films fabricated by spray-coating. a) CNT/TPE composite fabricated by spray coating. Reproduced with permission.[138] Copyright 2017, Wiley-VCH.b) SWNT/PDMS composite fabricated by spray coating. Reproduced with permission.[139] Copyright 2015, Springer Nature.

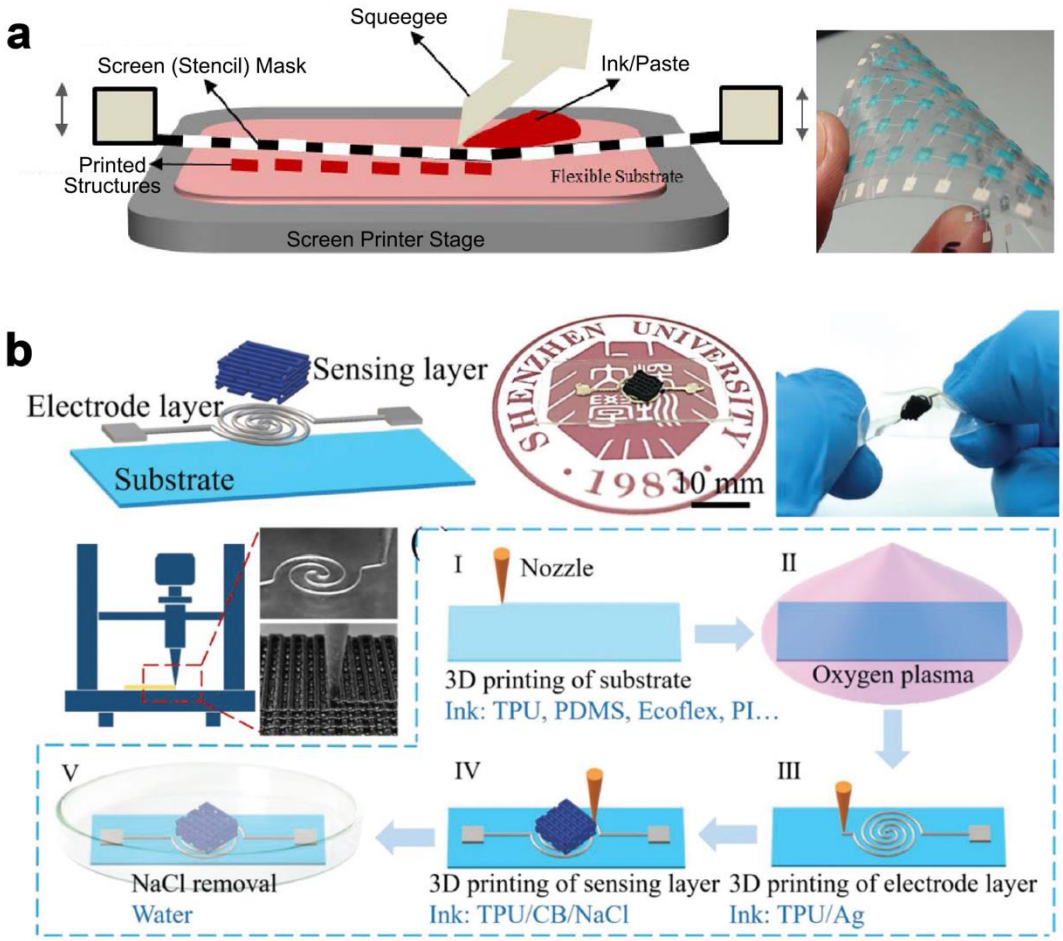

Figure 8. a) Schematic diagram showing the screen printing MWCNT/PDMS composite on flexible substrate and the photograph of the related flexible temperature sensor arrays. b) Schematic illustrations showing the 3D printed CB/TPU composite film for strain sensors. Reproduced with permission.[63] Copyright 2019, Wiley-VCH.

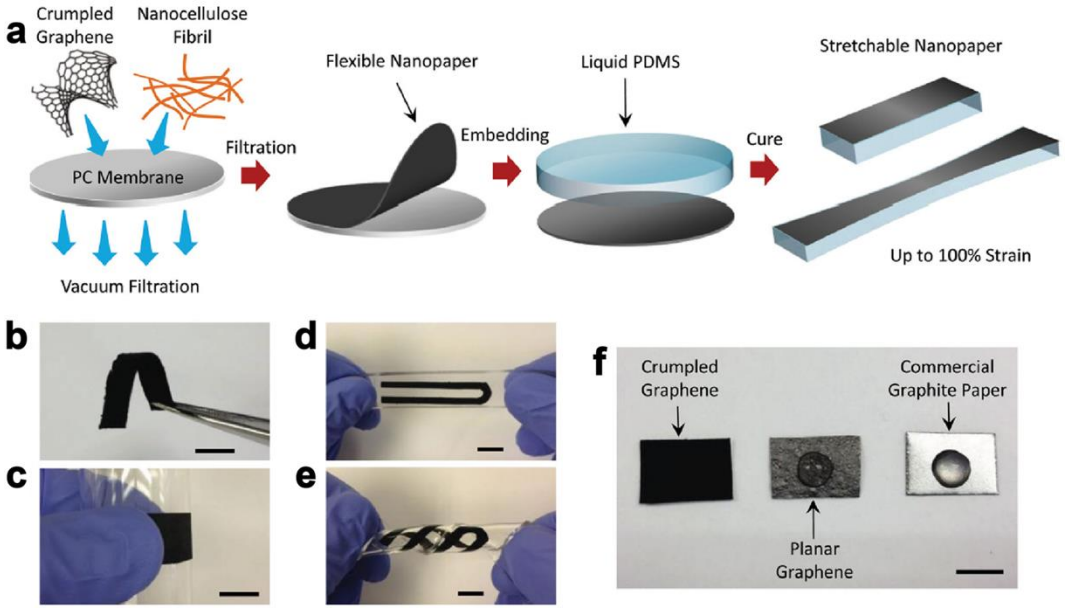

Figure 9. a) Schematic fabrication procedures of stretchable graphene/PDMS nanopapers. b-e) Photographs of the free-standing flexible nanopaper showing excellent flexibility and stretchability. f) Water adsorption comparison of crumpled graphene paper, planar graphene paper and commercial graphite paper, demonstrating the porous structure of graphene/PDMS nanopaper. Reproduced with permission.[153] Copyright 2014, Wiley-VCH.

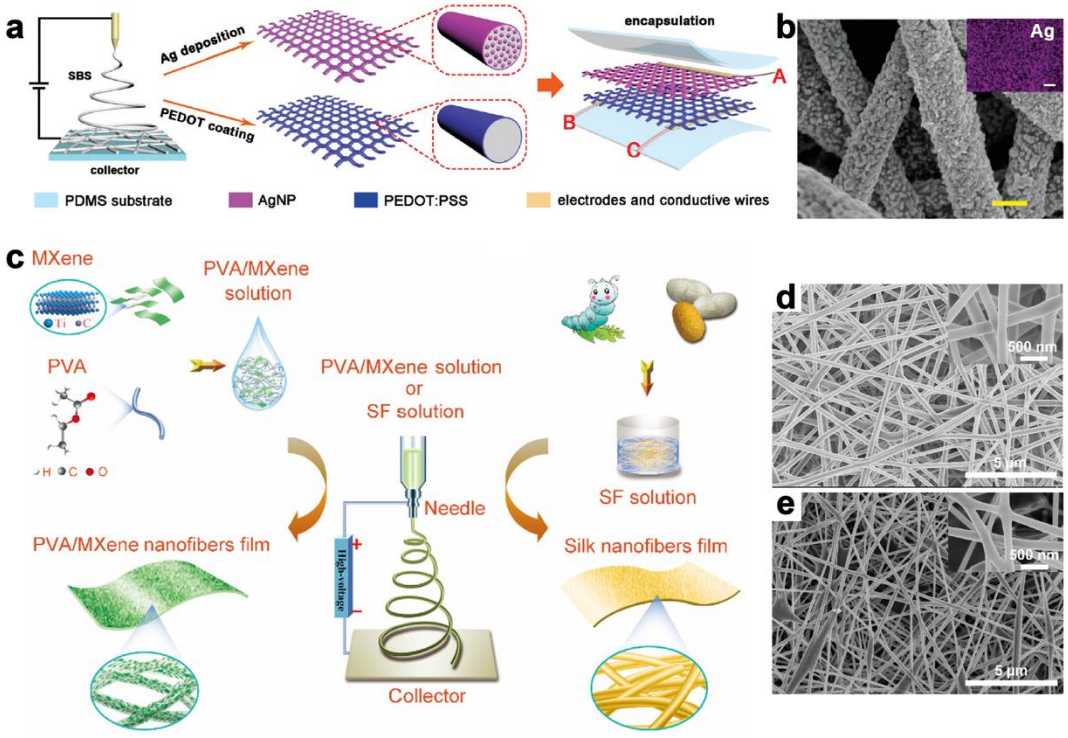

Figure 10. Functional composite fibers deposited by electrospinning. a) AgNP/SBS and PEDOT:PSS/SBS composite fibers for bimodal sensors. b) SEM image of AgNP/SBS composite fibers showing the uniform dispersion of AgNPs. Reproduced with permission.[83] Copyright 2019, Royal Society of Chemistry. c) Schematic illustrations showing PVA/MXene composite fibers for energy harvesters. d,e) SEM images of pure PVA nanofibers and PVA/MXene composite nanofibers. c–e) Reproduced with permission.[158] Copyright 2019, Elsevier.

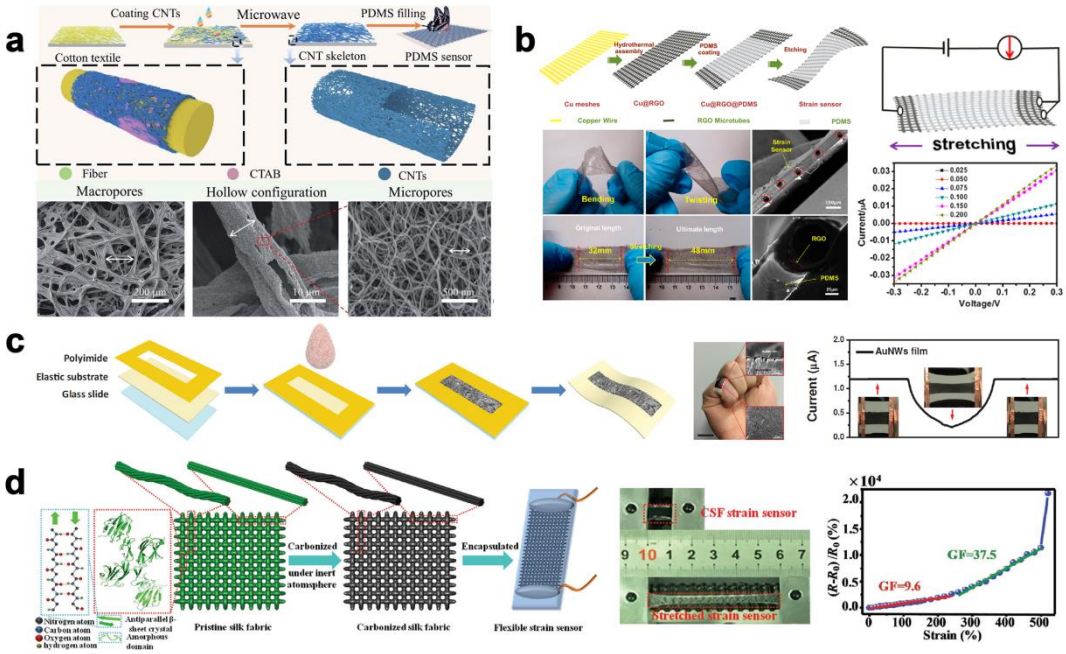

Figure 11. Strain sensors based on functional polymer composites. a) A CNT/PDMS composite based strain sensor. Reproduced with permission.[75] Copyright 2021, Royal Society of Chemistry. b) rGO/PDMS based strain sensor. Reproduced with permission.[181] Copyright 2015, American Chemical Society. c) AuNWs film based strain sensor. Reproduced with permission.[182] Copyright 2015, Wiley-VCH. d) Carbonized silk fabric/PDMS based strain sensor. Reproduced with permission.[183] Copyright 2016, Wiley-VCH.

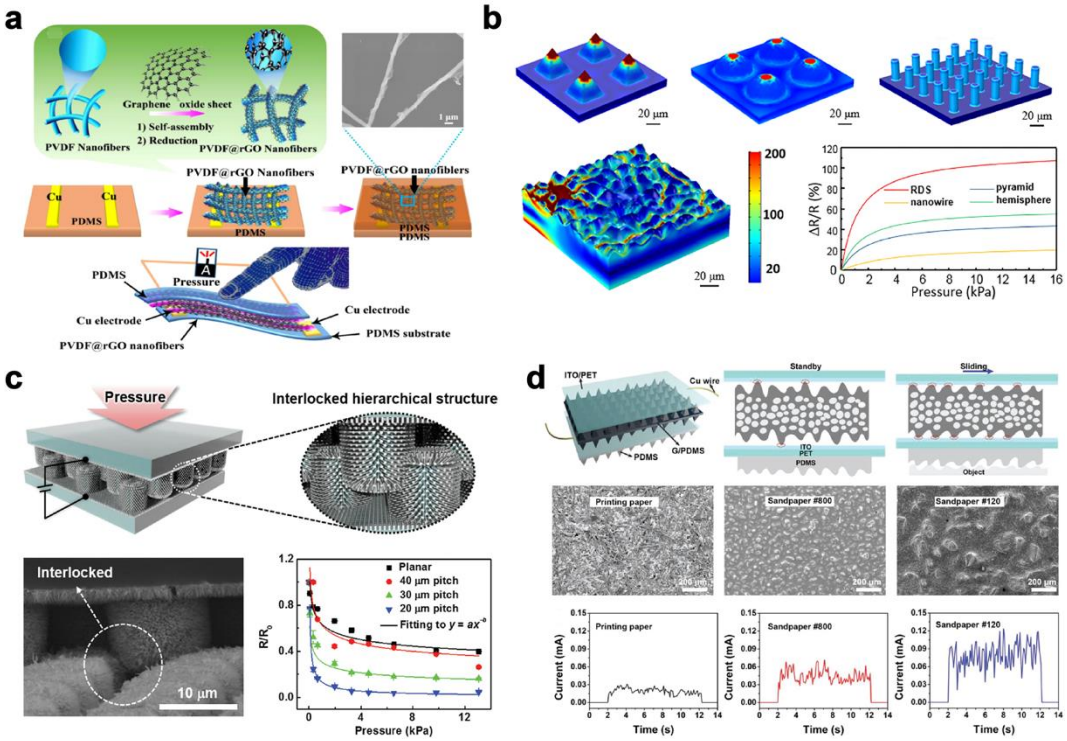

Figure 12. Flexible pressure sensors based on functional polymer composites. a) A rGO/PVDF nanofiber composite based flexible pressure sensor. Reproduced with permission.[189] Copyright 2016, Elsevier. b) Simulation of the sensing mechanism for GO/PDMS composite based pressure sensor. Reproduced with permission.[34] Copyright 2018, American Chemical Society. c) ZnO NW/PDMS composite based pressure sensor with an interlocked hierarchical structure. Reproduced with permission.[30] Copyright 2015, Wiley-VCH. d) Hierarchically structured Graphite/PDMS composite based pressure sensor in detecting the texture roughness. Reproduced with permission.[66] Copyright 2019, Wiley-VCH.

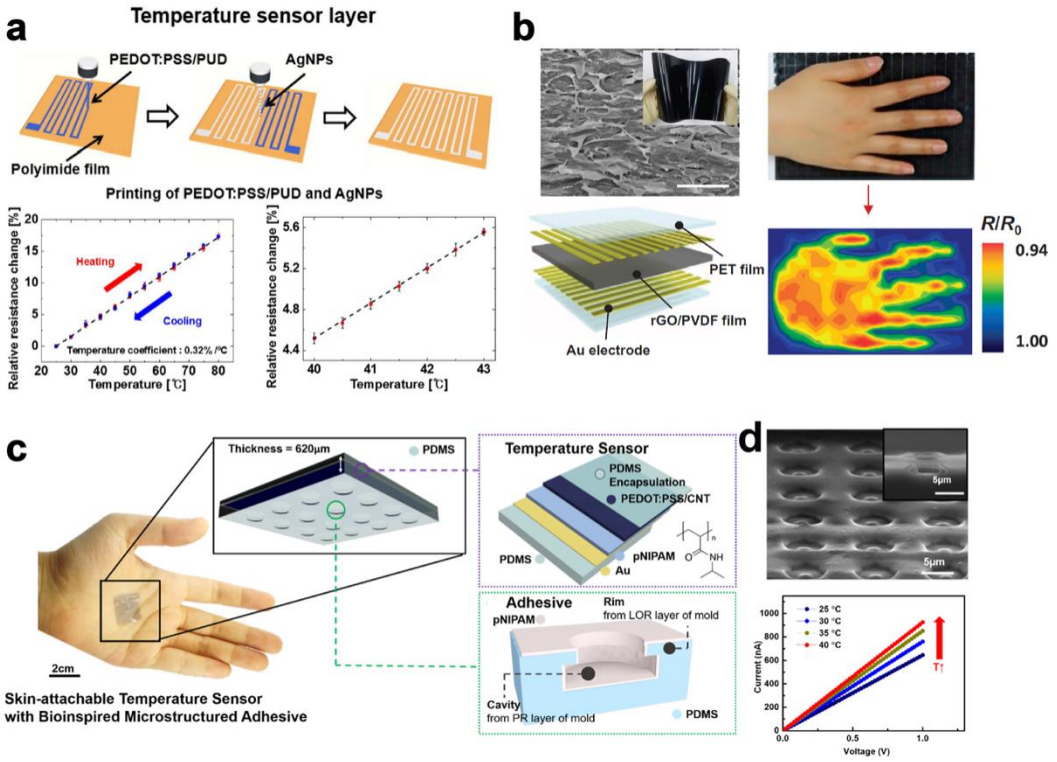

Figure 13. Thermistor temperature sensors with functional polymer composite films. a) A PEDOT:PSS/PUD/AgNP composite film based temperature sensor developed by inkjet printing. Reproduced with permission.[196] Copyright 2017, Elsevier. b) Temperature sensor arrays based on rGO/PVDF composite film for mapping the spatial temperature distribution. Reproduced with permission.[31] Copyright 2015, American Association for the Advancement of Science. c) An attachable temperature sensor based on a bio-inspired composite film. d) SEM image of the bio-inspired composite film and the current response to temperature. Reproduced with permission.[197] Copyright 2018, American Chemical Society.

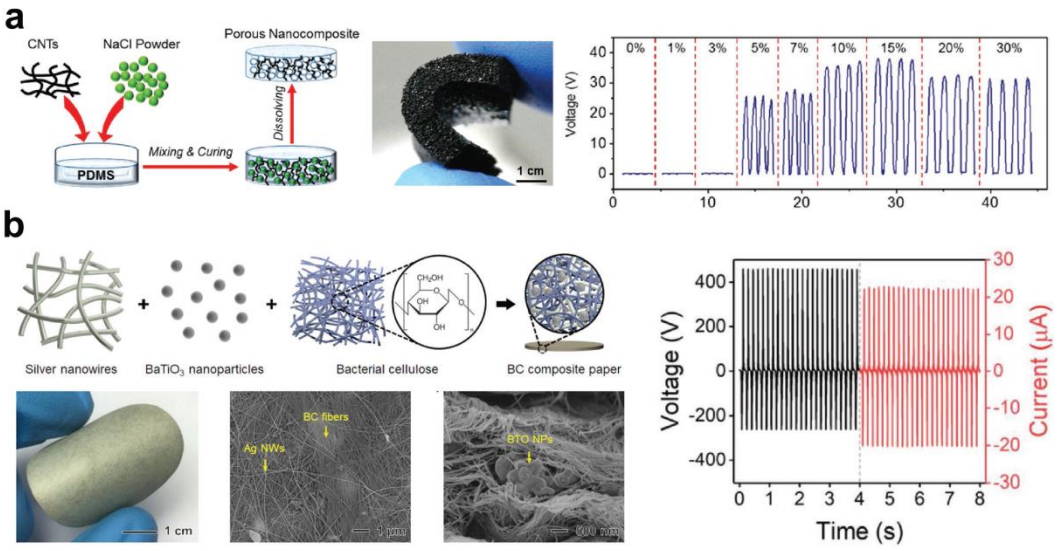

Figure 14. Energy harvesters based on functional polymer composites. a) A stretchable triboelectric nanogenerator based on porous CNTs/PDMS composite. Reproduced with permission.[207] Copyright 2017, Wiley-VCH. b) A stretchable triboelectric nanogenerator with a conductive ferroelectric cellulose composite paper. Reproduced with permission.[208] Copyright 2019, Wiley-VCH.

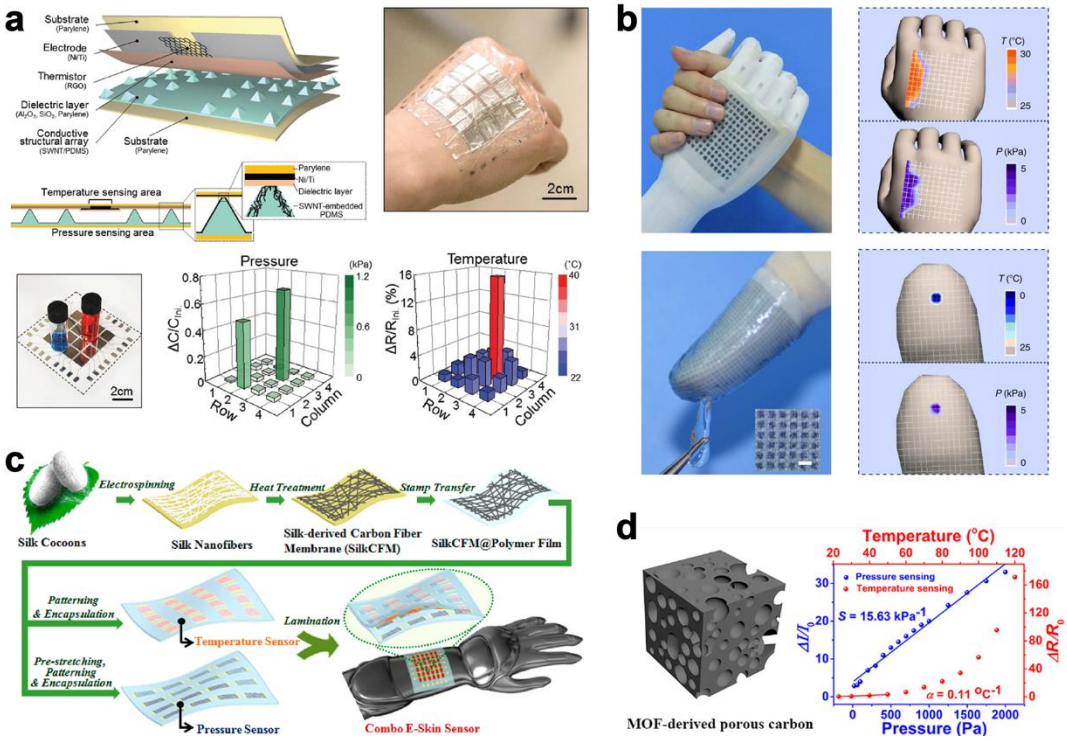

Figure 15. Temperature/pressure bimodal sensors based on functional polymer composites. a) Schematic illustration of stimulus-discriminating and linearly sensitive bimodal sensor. Reproduced with permission.[190] Copyright 2018, Wiley-VCH. b) Self-powered temperature/pressure bimodal sensors with organic thermoelectric composite. Reproduced with permission.[209] Copyright 2015, Springer Nature. c) Silk-derived carbon fiber/PDMS membrane based temperature/pressure sensor. Reproduced with permission.[184] Copyright 2017, American Chemical Society. d) MOF-derived porous carbon/PDMS composite based bimodal sensor. Reproduced with permission.[213] Copyright 2018, American Chemical Society.

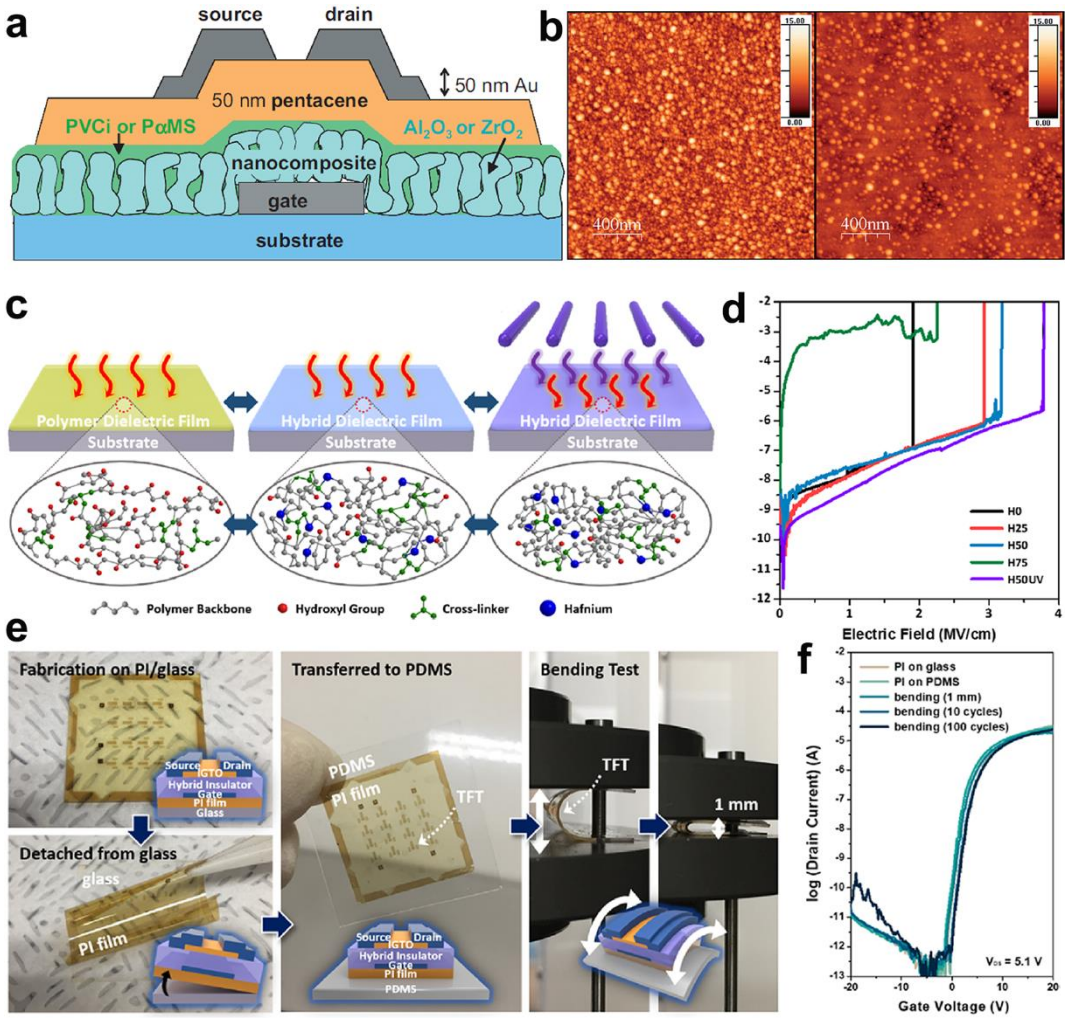

Figure 16. a) Cross-sectional view of OFET geometry. AFM images of bare ZrO_2 and ZrO_2/PaMS nanocomposite film surfaces. Reproduced with permission.[219] Copyright 2007, Wiley-VCH. b) Schematic illustrations of the chemical structures of the H0, H50, and H50UV polymer-based dielectric films. Breakdown E-field characteristics of the capacitors based on various dielectrics and bending test of the transistors. Reproduced with permission.[220] Copyright 2019, American Chemical Society.

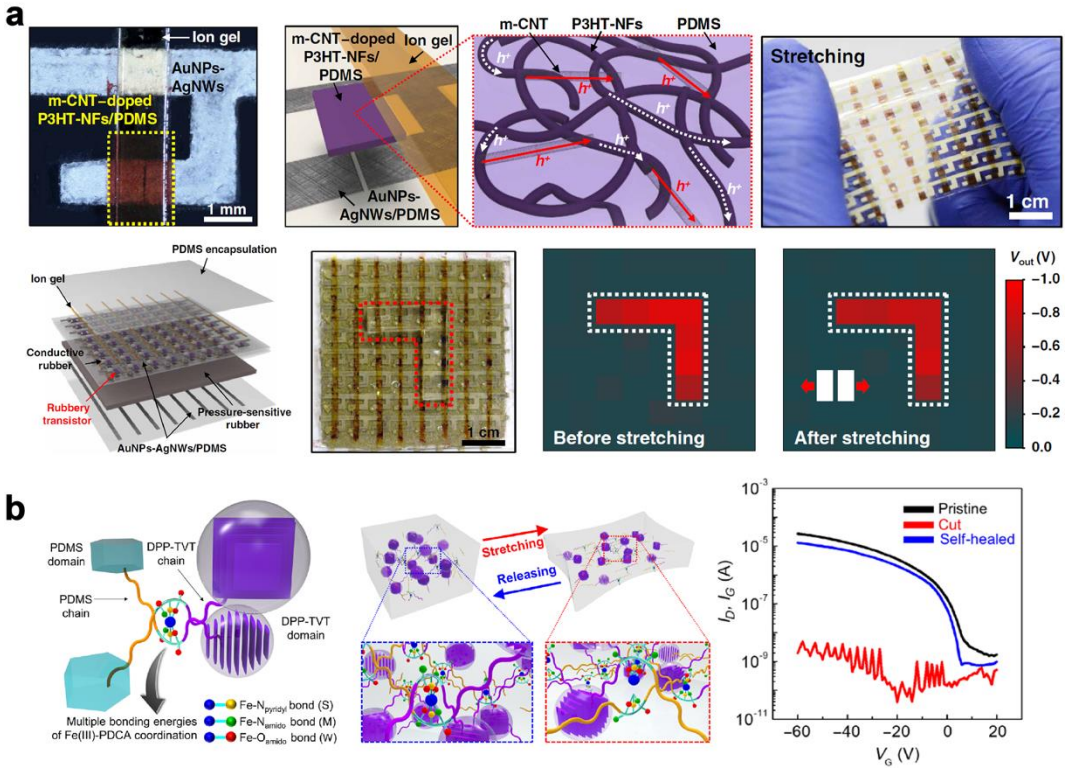

Figure 17. a) Fully rubbery integrated electronics with intrinsically stretchable polymer composite as semiconductors. Reproduced with permission.[223] Copyright 2019, American Association for the Advancement of Science. b) Stretchable self-healable semiconducting polymer film based active-matrix strain-sensing array. Reproduced with permission.[224] Copyright 2019, American Association for the Advancement of Science.

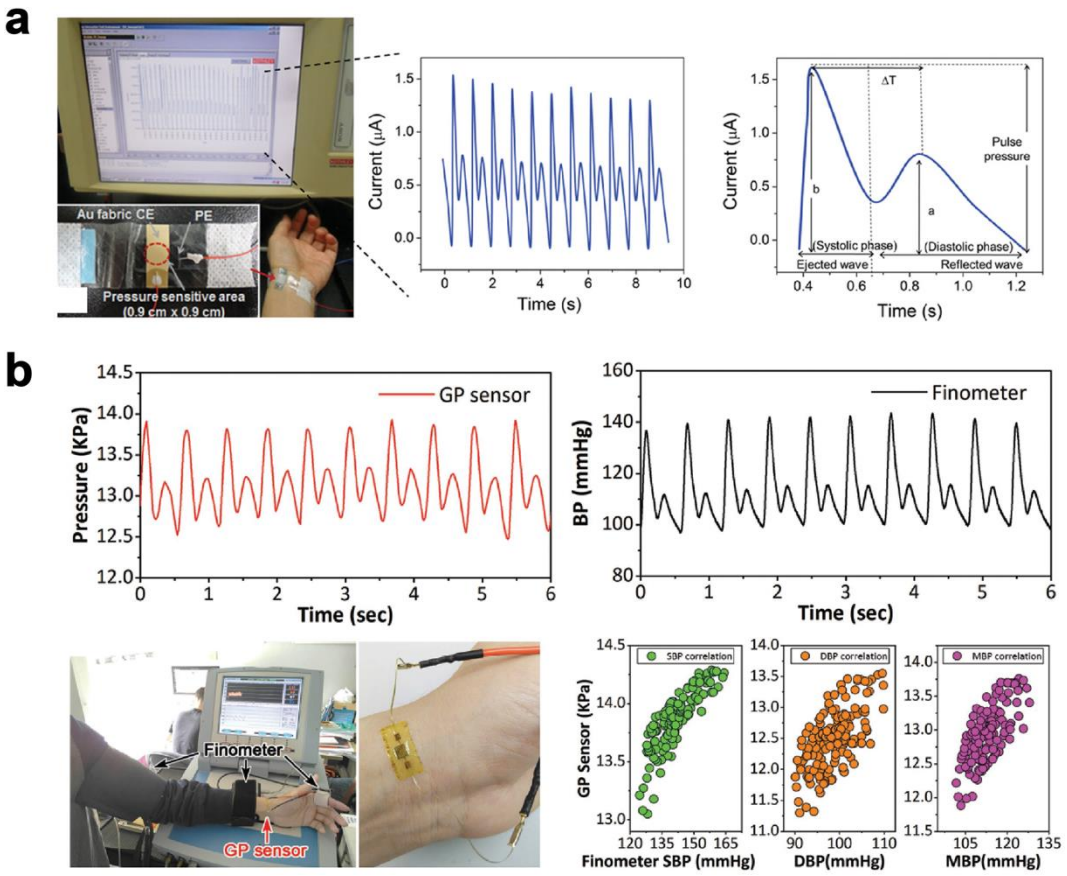

Figure 18. a) Blood pressure monitoring using a pressure sensor based on PEDOT:PSS/PUD composite. Reproduced with permission.[33] Copyright 2014, Wiley-VCH. b) Blood pressure sensor based on graphene/PDMS composite for detecting wrist pulses and blood pressure. Reproduced with permission.[225] Copyright 2017, Wiley-VCH.

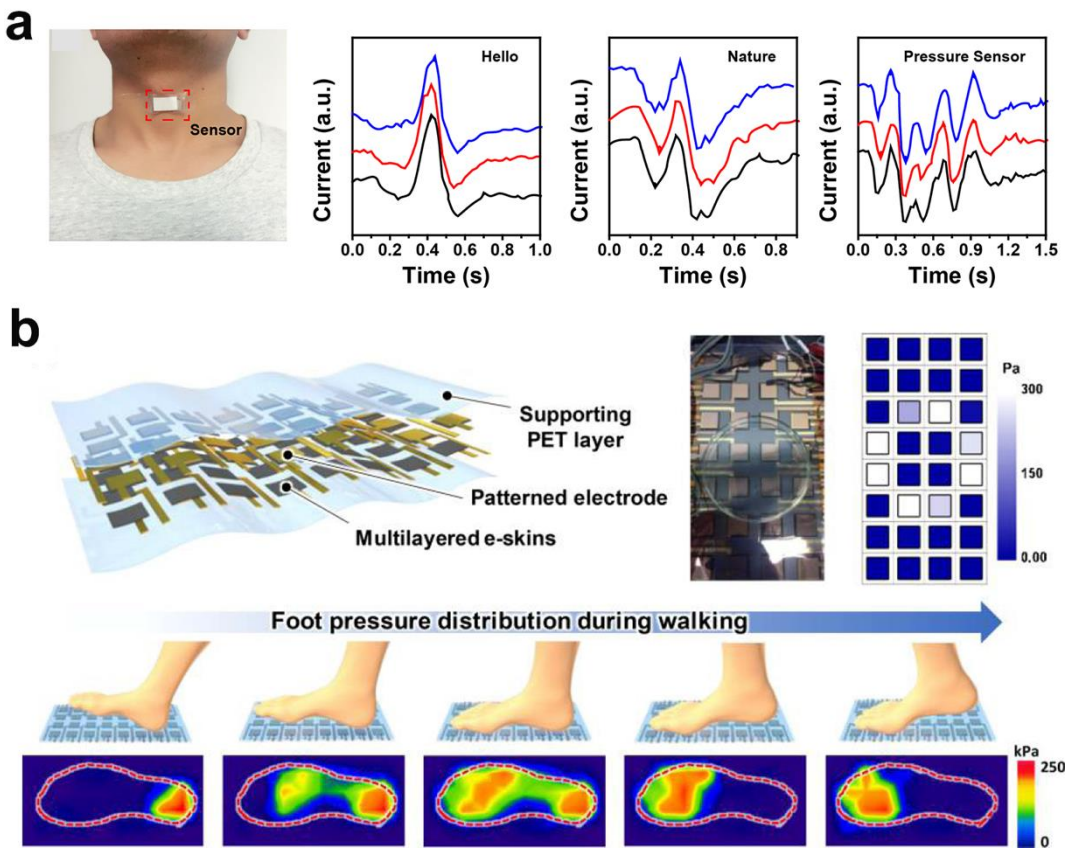

Figure 19. a) Hierarchically structured graphite/PDMS composite based pressure sensor for voice recognition. Reproduced with permission.[65] Copyright 2018, American Chemical Society. b) rGO/PVDF based E-skin for mapping the plantar pressure distribution. Reproduced with permission.[6] Copyright 2018, American Chemical Society.

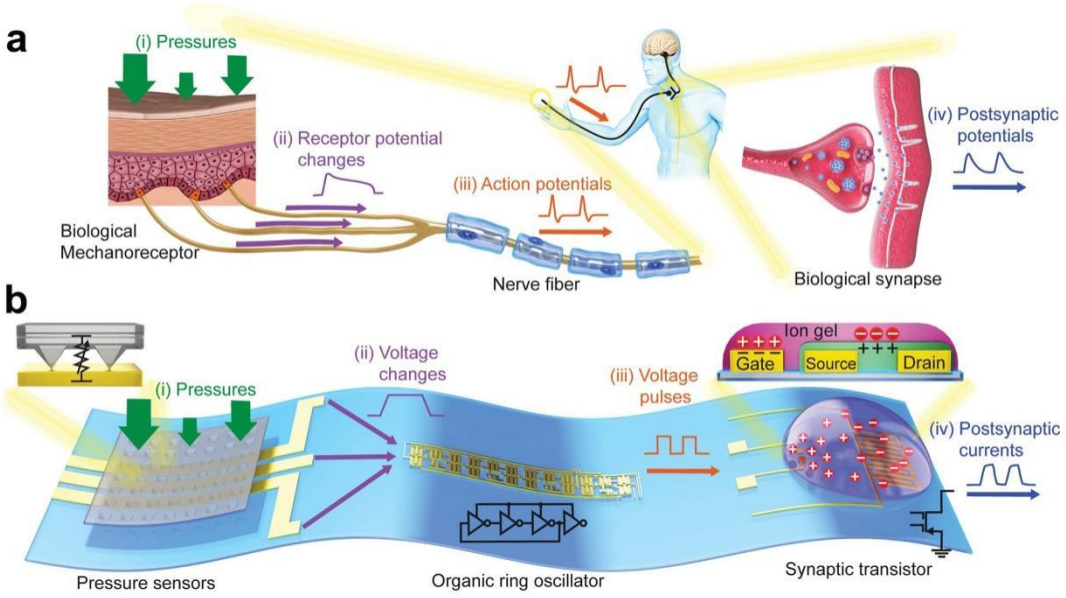

Figure 20. a) Schematic illustrations showing a biological artificial afferent nerve system. b) An artificial afferent nerve including pressure sensors, ring oscillator, and a transistor. Reproduced with permission.[232] Copyright 2018, American Association for the Advancement of Science.

Table 1. The performance of FPC based pressure sensors

Materials	Sensitivity (kPa^{-1})	Low limit (Pa)	Up limit (kPa)	Response time (ms)	Durability (cycles)	Ref.
rGO/PVDF	47.7	1.3	353	20	5000	[6]
(Ag NFs)/SF	5.5	35	700	NA	7000	[5]
MXene/rGO	22.56	10	3.5	<200	>10 000	[13]
graphene/PDMS	14	1	12	30	10 000	[32]
rGO/PDMS	25.1	16	40	80	3000	[34]
CNT/porous PDMS	0.02	10	1200	8	10 000	[40]
SSNPs/PU	2.46	300	10	30	1000	[44]
PEDOT:PSS/PDMS	851	34	20	0.15	18 000	[50]
AgNWs/PDMS	0.03	NA	6	20	>1000	[55]
CB/TPU	5.54	10	800	18	10000	[63]
Graphite/PDMS	64.3	0.9	10	8	100 000	[65]
Graphite/porous PDMS	245	5	120	4	>1000	[66]
aPANF/GA	28.62	3	14	37	2600	[69]
rGO/PU	0.26	5	10	NA	>10000	[70]
CNT/PDMS	15.1	0.2	30	40	NA	[77]
AuNWs/PDMS	23	NA	3	10	10 000	[93]
Ag/PEDOT:PSS/SBS	1185.8	2.4	80	16	5000	[83]
AgNWs/Graphene/PANFs	134	3.7	75	20	8000	[166]
AgNWs/ MXene	645.69	1.25	9	60	1000	[168]
MXene/PVDF-TrFE	0.51	1.5	400	150	10 000	[170]

rGO: reduced graphene oxide; PVDF: poly(vinylidene fluoride); Ag NFs: silver Nanofibers; SF: silk fabric; PDMS: polydimethylsiloxane; CNT: carbon nanotubes; SSNPs: sea-urchin shaped metal nanoparticles; CB: carbon blacks; TPU: thermoplastic urethane elastomer; aPANF/GA: anofiber reinforced graphene aerogel; PU: polyurethane; SBS: poly(styrene-block-butadiene-block-styrene); polyamide nanofibers (PANFs), PVDF-TrFE: poly(vinylidene fluoride-trifluoroethylene).

Qi-Jun Sun is currently a Lecture at School of Physics and Optoelectric Engineering, Guangdong University of Technology. He received his Ph. D degree in physics and materials science from City University of Hong Kong in 2017. After graduation, he worked in the Department of Materials Science and Engineering at City University of Hong Kong as a research fellow and then joined Guangdong University of Technology in 2021. His main research interests include functional electronic devices, self-powered electronics, and wearable sensors.

Zhenhua Tang is currently an Associate Professor at School of Physics and Optoelectric Engineering, Guangdong University of Technology. He received PhD degree from Xiangtan University in 2015. He worked as a research associate at Department of Physics, The University of Hong Kong from December, 2015 to January, 2017, and worked as a research fellow at Department of Materials Science & Engineering, National University of Singapore from February, 2017 to May, 2018. He has authored and/or co-authored more than 63 papers in the pier-reviewed journals. His primary scientific interests cover the fields of flexible electronic device, sensors, ferroelectrics, and multiferroics.

Roy Vellaisamy is a Professor of Intelligent systems at the James Watt School of Engineering, University of Glasgow. He works on multidisciplinary research blending device physics with materials chemistry and electronic engineering. He has published more than 200 articles in journals such as *Nature Communications, Advanced Materials, Advanced Functional Materials* etc.. In addition, he has 21 US/Intrenational/Chinese patents. He has led several applied projects on sensors and neuromorphic memories worth of several million dollars and licensed the technologies to industries. In 2019, he received gold medal for his *"Sensor Platform" at the International Exhibition of Inventions Geneva.*

Functional polymer composite (FPC) material based E-skin shows superiorities in light-weight, high sensitivity, excellent flexibility and stretchability. With the excellent properties, FPC based E-skin shows great potential applications in health monitoring and artificial intelligence, including wrist pulse monitoring, body temperature monitoring, human motion detection, prosthetics and robotics as well.

Keyword: functional composites, flexible sensors, E-skin, health monitoring, artificial intelligence

Qi-Jun Sun, Qin-Teng Lai, Zhenhua Tang*, Xin-Gui Tang, Xin-Hua Zhao*, and Vellaisamy A. L. Roy*

Advanced Functional Composite Materials Towards E-skin for Health Monitoring and Artificial Intelligence

Table of Contents